

CONFIDENTIAL

Copy 260  
RM L53H27

NACA RM L53H27



# RESEARCH MEMORANDUM

LOW-SPEED STATIC STABILITY AND CONTROL CHARACTERISTICS OF  
 A  $\frac{1}{4}$ -SCALE MODEL OF THE BELL X-1 AIRPLANE EQUIPPED  
 WITH A 4-PERCENT-THICK, ASPECT-RATIO-4,  
 UNSWEPT WING

By William C. Moseley, Jr., and Robert T. Taylor

Langley Aeronautical Laboratory  
 Langley Field, Va.

CLASSIFIED DOCUMENT

This material contains information affecting the National Defense of the United States within the meaning of the espionage laws, Title 18, U.S.C., Secs. 793 and 794, the transmission or revelation of which in any manner to an unauthorized person is prohibited by law.

NATIONAL ADVISORY COMMITTEE  
 FOR AERONAUTICS

WASHINGTON

November 2, 1953

CLASSIFICATION CHANGED TO UNCLASSIFIED  
 AUTHORITY: NACA RESEARCH ABSTRACT NO. 146  
 EFFECTIVE DATE: AUGUST 16, 1957  
 WHL

CONFIDENTIAL

## NATIONAL ADVISORY COMMITTEE FOR AERONAUTICS

## RESEARCH MEMORANDUM

## LOW-SPEED STATIC STABILITY AND CONTROL CHARACTERISTICS OF

A  $\frac{1}{4}$ -SCALE MODEL OF THE BELL X-1 AIRPLANE EQUIPPED

WITH A 4-PERCENT-THICK, ASPECT-RATIO-4,

UNSWEPT WING

By William C. Moseley, Jr., and Robert T. Taylor

## SUMMARY

An investigation was made in the Langley 300 MPH 7- by 10-foot tunnel to determine the low-speed static stability and control characteristics of a  $\frac{1}{4}$ -scale model of the Bell X-1 airplane equipped with a 4-percent-thick, aspect-ratio-4 wing. Tests were also made to determine the optimum flap deflection for a slotted flap.

Results of the tests indicated that the model had elevator-fixed longitudinal stability amounting to a static margin of about 0.12 mean aerodynamic chord for the flaps-retracted configuration and a static margin of about 0.04 mean aerodynamic chord for the flaps-deflected configuration, both configurations becoming extremely stable near the stall. The model possess static lateral and directional stability throughout the usable angle-of-attack range. The existing elevator and rudder provided satisfactory control generally similar to the original  $\frac{1}{4}$ -scale model of the airplane. The aileron retained its effectiveness which agreed with predicted effectiveness up to near the stall. This effectiveness was generally unaffected by deflecting the flaps. The optimum flap deflection was  $35^\circ$ .

## INTRODUCTION

Extensive research has indicated that airfoil thickness is of primary importance in the performance of aircraft designed to operate in

CONFIDENTIAL

the transonic and supersonic speed ranges. At the request of the National Advisory Committee for Aeronautics, a 4-percent-thick wing is being incorporated into the Bell X-1 research airplane. The use of thin sections, in general, requires an accompanying change in aspect ratio or taper ratio, or both from purely structural considerations.

The present paper presents the results of an investigation to determine the effect, if any, that a change in wing thickness and an associated change in aspect ratio would have on the low-speed static stability and control characteristics of the Bell X-1 airplane. The investigation was made in the Langley 300 MPH 7- by 10-foot tunnel with a  $\frac{1}{4}$ -scale model

of the Bell X-1 airplane equipped with a wing of aspect ratio 4, taper ratio 0.5,  $0^{\circ}$  sweepback of the 0.40 chord line, and a modified NACA 64A004 airfoil section. The wing had a slotted flap of about 0.50 semispan and an aileron of 0.30 semispan.

#### COEFFICIENTS AND SYMBOLS

The system of axes used together with an indication of positive forces, moments, and angles is presented in figure 1. Moments are given about the center-of-gravity location shown in figure 2(a), (20 percent of the mean aerodynamic chord of the wing). The coefficients and symbols used in this paper are defined as follows:

$C_L$	lift coefficient, $Lift/qS$
$C_D$	drag coefficient, $Drag/qS$
$C_Y$	lateral-force coefficient, $Y/qS$
$C_l$	rolling-moment coefficient, $L/qSb$
$C_n$	yawing-moment coefficient, $N/qSb$
$C_m$	pitching-moment coefficient, $M/qS\bar{c}$
$C_{h_a}$	aileron hinge-moment coefficient, $H/q2M'$
$X$	longitudinal force along X-axis (drag equals $-X$ when $\beta = 0$ ), lb
$Y$	lateral force along Y-axis, lb

Z	force along Z-axis (lift equals -Z), lb
L	rolling moment about X-axis, ft-lb
N	yawing moment about Z-axis, ft-lb
M	pitching moment about Y-axis, ft-lb
H	aileron hinge moment about hinge line, ft-lb
q	free-stream dynamic pressure, $\frac{1}{2}\rho V^2$ , lb/sq ft
M'	area moment of aileron rearward of hinge line about hinge line, ft <sup>3</sup>
S	wing area, sq ft
c	mean aerodynamic chord, ft
A	aspect ratio, $b^2/S$
c	local wing chord, ft
b	wing span, ft
pb/2V	helix angle of roll, radius
V	free-stream velocity, ft/sec
p	angular velocity in roll, radians/sec
$\rho$	mass density of air, slugs/cu ft
$F_w$	wheel force, based on a wheel radius of 0.542 feet, lb
$\alpha$	angle of attack of fuselage center line, deg
$\beta$	angle of sideslip, deg
$i_t$	angle of incidence of horizontal tail with respect to fuselage center line, deg
$\delta$	angle of control deflection, deg
$C_{L\alpha}$	rate of change of $C_L$ with $\alpha$ at a constant $\beta$ , $\left(\frac{\partial C_L}{\partial \alpha}\right)_{\beta}$

$C_{l_\delta}$	rate of change of $C_l$ with $\delta$ at a constant $\alpha$ , $\left(\frac{\partial C_l}{\partial \delta}\right)_\alpha$
$C_{l_\beta}$	rate of change of $C_l$ with $\beta$ at a constant $\alpha$ , $\left(\frac{\partial C_l}{\partial \beta}\right)_\alpha$
$C_{n_\beta}$	rate of change of $C_n$ with $\beta$ at a constant $\alpha$ , $\left(\frac{\partial C_n}{\partial \beta}\right)_\alpha$
$C_{Y_\beta}$	rate of change of $C_Y$ with $\beta$ at a constant $\alpha$ , $\left(\frac{\partial C_Y}{\partial \beta}\right)_\alpha$
$C_{h_{a_\alpha}}$	rate of change of $C_{h_a}$ with $\alpha$ at a constant $\delta$ , $\left(\frac{\partial C_{h_a}}{\partial \alpha}\right)_\delta$
$C_{h_{a_\delta}}$	rate of change of $C_{h_a}$ with $\delta$ at a constant $\alpha$ , $\left(\frac{\partial C_{h_a}}{\partial \delta}\right)_\alpha$
$\frac{\partial C_m}{\partial i_t}$	rate of change of $C_m$ with $i_t$ at a constant $\alpha$

## Subscripts:

e	elevator
r	rudder
f	flap
a	aileron
t	total

All slopes were measured in the vicinity of  $\alpha$ ,  $\beta$ ,  $\delta = 0$ .

## MODEL AND APPARATUS

The physical characteristics of the  $\frac{1}{4}$  - scale model of the Bell X-1 airplane used during the present investigation are presented in figure 2(a). For comparison, the characteristics of a  $\frac{1}{4}$  - scale model of the original

Bell X-1 airplane are shown in figure 2(b). The original model had a 10-percent-thick wing with an aspect ratio of 6 and a taper ratio of 0.5. The wing used in the present investigation had an aspect ratio of 4, a taper ratio of 0.5, a modified NACA 64A004 airfoil section,  $0^\circ$  sweepback of the 0.40 chord line and had an area equal to the wing of the original Bell X-1 model. The airfoil section was altered rearward of the 0.70 chord line to give a constant trailing-edge thickness of  $\frac{1}{16}$  inch with straight contours being faired into the airfoil contour at the 0.70 chord line. The wing had a steel spar covered with mahogany which was wrapped with Fiberglas and Paraplex. The flaps and aileron were machined of aluminum. Photographs showing the model mounted on the single support strut of the Langley 300 MPH 7- by 10-foot tunnel are presented as figure 3.

Details of the flap and ailerons are shown in figure 4. The 0.25c aileron had a  $0.20c_a$  overhang balance and extended from  $0.68b/2$  to  $0.98b/2$ . The ailerons had straight sides with a radius nose. A gap of  $\frac{1}{64}$  inch between the aileron nose and the wing was left unsealed for

these tests. Also included was an electric strain gage installed at the inboard end of the right aileron to give an indication of the aileron hinge moments. The 0.27c single slotted flap had straight sides and extended inboard of the aileron to the juncture of the wing and fuselage (approximately  $0.188b/2$ ). There was no fillet at the wing-fuselage juncture. The flap nose had an elliptical shape on the upper surface and a radius on the lower surface. (See fig. 4(b).) The flap was hinged externally at the  $0.748c$  position and  $0.022c$  below the chord plane. Only one flap-hinge location was tested and no attempt was made to evaluate the effect of varying the slot shape or the flap-hinge location.

#### TESTS AND CORRECTIONS

The tests were made in the Langley 300 MPH 7- by 10-foot tunnel at a dynamic pressure of 25.86 pounds per square foot, which corresponds to a Mach number of approximately 0.13 and a Reynolds number of about  $1.2 \times 10^6$  based on a mean aerodynamic chord of 1.48 feet.

The angles of attack, drag coefficients, and pitching-moment coefficients have been corrected for jet-boundary effects determined by the methods of reference 1. Corrections for blocking caused by the model and its wake have been applied according to the methods of reference 2. Horizontal buoyancy on the model due to longitudinal pressure gradient, and tunnel air-flow misalignment have also been accounted for in the computation of the test data.

Tare corrections to account for that portion of the forces and moments attributable to the support strut have not been applied to the data. Estimates made from previous investigations of a similar model indicated that tare corrections were small except for the drag coefficient which would be reduced by about 0.01 at zero lift.

## RESULTS AND DISCUSSION

### Presentation of the Data

The following table gives a brief summary of the figures presented:

	Figure
Effect of horizontal tail setting . . . . .	5 and 6
Static margin . . . . .	. . . . . 7
Elevator effectiveness . . . . .	8 and 9
Elevator and tail incidence required for trim . . . . .	. . . . . 10
Effect of flap deflection . . . . .	. . . . . 11
Flap effectiveness . . . . .	. . . . . 12
Characteristics in sideslip . . . . .	13 and 14
Lateral stability parameters . . . . .	. . . . . 15
Aileron characteristics . . . . .	16 and 17
Helix angle and wheel force for steady roll . . . . .	. . . . . 18
Effect of rudder deflection . . . . .	19 and 20
Rudder and aileron required for steady sideslip . . . . .	. . . . . 21

### Longitudinal Stability and Control

Longitudinal stability. - Figure 7 summarizes the longitudinal stability characteristics of the model of the present paper. The static margin in percent  $\bar{c}$  is presented for flap deflections of  $0^\circ$  and  $35^\circ$  along with the data for the flap-retracted configuration of the original Bell X-1 model. The static margin of the subject model was about  $0.12\bar{c}$  up to about 0.6 lift coefficient; above  $C_L = 0.6$ , there was an abrupt increase in the static margin. Data obtained in the Langley 7- by 10-foot tunnel indicate that the static margin of the original X-1 model was generally constant ( $0.09\bar{c}$  up to  $C_L = 0.6$ ). Deflecting the slotted flap reduced the static margin to about  $0.04\bar{c}$ , which increased rapidly as the stall was approached.

The variation of pitching-moment coefficient with lift coefficient of figures 6, 8, and 9 show curves which are generally linear and stable up to the stall, with a stable break at the stall at horizontal tail settings and elevator deflections near trim and balance.

Longitudinal control. - The horizontal-tail effectiveness parameter  $\partial C_m / \partial i_t$  for the flap-retracted configuration was about -0.03 and for the flap deflected-configuration, about -0.027. Although these values are somewhat smaller than for the original X-1 model ( $\partial C_m / \partial i_t = -0.035$ ;  $\delta_f = 0^\circ$  and  $\delta_f = 60^\circ$ ), it should be remembered that, although the tail length was the same, the mean aerodynamic chord was larger for the present model.

The data of figure 8 show the aerodynamic characteristics for the flap-retracted condition. The data of figure 8(b) indicate that the elevator was sufficient to maintain a lift coefficient of 0.70 at an angle of attack of  $12^\circ$ , a stabilizer setting of  $i_t = 3.8^\circ$ , and a  $20^\circ$  elevator deflection.

The data of figure 9 show the aerodynamic characteristics for the landing condition. The data of figure 9(b) indicate that the elevator was sufficient to maintain a lift coefficient of 1.04 at an angle of attack of  $6^\circ$  with a horizontal-tail setting of  $2.4^\circ$  and an elevator deflection of  $-5^\circ$ .

Figure 10 summarizes the longitudinal-control characteristics of the model and indicates a moderate change in elevator deflection or stabilizer setting is required to balance the model through most of the lift-coefficient range.

#### High Lift Devices

The plain-wing tail-off lift-curve slope (fig. 5) was about 0.068 and compares well with the theoretical wing-alone lift-curve slope (0.064) as determined from reference 3. It is felt that the contribution of the fuselage is significant in raising the lift-curve slope of the model and may account for some of the discrepancy between experiment and theory.

The lift data of figure 11 indicate that the lift-curve slope of the complete model varied between 0.074 at  $\delta_f = 0$  to 0.066 at  $\delta_f = 30^\circ$ .

The variation of lift coefficient with flap deflection (fig. 12) indicates that the optimum flap deflection is  $35^\circ$  for the slot tested. This flap deflection yields an increment in lift coefficient of 0.64 at an angle of attack of  $4^\circ$ . Although the flap at  $\alpha = 0^\circ$  and  $\alpha = 4^\circ$  yields a slightly higher lift coefficient for flap deflections above  $35^\circ$  the corresponding increase in drag is excessively high. The values of  $C_{L_{max}}$  presented are peak values or were taken just beyond the point where an abrupt decrease in lift-curve slope occurred for flap deflections where no definite peak existed.

The landing speed of the X-1 airplane can be determined if an empty weight of 7000 pounds is assumed for the airplane. (All unexpended fuel is jettisoned before landing.) From figure 9(b) a balanced lift coefficient of about 1.03 is obtained for an angle of attack of  $4^{\circ}$ . The wing loading would be 53.8 pounds per square foot and the landing speed would be about 145 miles per hour.

#### Lateral and Directional Stability

The data of figure 15 indicate that the model possessed both static lateral and static directional stability that was generally fairly constant with increase in lift coefficient. The stability parameters obtained from figures 13 and 14 agree very well with the values in figure 15 obtained at  $\beta = \pm 5^{\circ}$ . The effective dihedral tended to increase near the higher lift coefficients for the flaps-retracted configuration, while for the flaps-deflected configuration the effective dihedral decreased slightly near the highest lift coefficient. The data for the original X-1 model with an aspect-ratio-6, 10-percent-thick wing yielded values generally the same at low lift coefficients but abrupt variations in effective dihedral occurred as the stall was approached. Deflecting the slotted flap had little effect on the static directional stability of the model.

#### Lateral and Directional Control

The data presented in figures 16 and 17 are for the right aileron deflected only. The tests were limited to approximate aileron travel on the actual airplane,  $\delta_a = \pm 12\frac{1}{2}^{\circ}$ . For the flap-retracted configuration (fig. 16), the aileron retained its effectiveness up to about  $\alpha = 10^{\circ}$  which is near the stall. (See fig. 5.) Above  $\alpha = 10^{\circ}$ , the aileron began to lose its effectiveness particularly for positive or down deflections. The aileron rolling effectiveness parameter  $C_{l\delta}$  was about -0.00127, which is about what would be expected for 0.256 flap-type control with a blunt overhang of  $0.20c_a$ . From the data of reference 4, an estimated value of  $C_{l\delta}$  was -0.0012. The data for the flap-deflected configuration (fig. 17) show that the aileron effectiveness parameter of the original model was larger than that of the present model,  $C_{l\delta} = -0.00157$  and  $C_{l\delta} = -0.00127$ , respectively; however, figure 18 shows the present model to have a rolling velocity per degree of aileron deflection approximately 20 percent higher than that of the original X-1 model.

The aileron hinge moments indicate that for the flap-retracted configuration the hinge-moment parameters were  $C_{h_{a_\alpha}} = -0.0038$ ,  $C_{h_{a_\delta}} = -0.0050$  and  $C_{h_{a_\delta}} = -0.0083$ . From reference 5, estimated values (flap retracted),  $C_{h_{a_\alpha}} = -0.0035$  and  $C_{h_{a_\delta}} = -0.0090$ , were obtained for a flap-type aileron with  $0.20c_a$  blunt overhang at low Mach numbers.

In order to compare estimated flight conditions with those of the original X-1 model, two flight conditions were selected and data for the conditions are given in table I. Condition I is for a heavily loaded, flap-retracted configuration, operating at a high lift coefficient. Condition II simulates an empty, flap-deflected, landing configuration. Figure 18 shows the rolling velocity, wheel force, and wing-tip helix angle plotted against aileron deflection at steady roll for conditions I and II for the model of the present investigation and condition I for the original X-1 model. The data indicated that, for a given aileron deflection, the present model has a stick force approximately 70 percent higher than that of the original X-1 model. However, for a given value of the rolling velocity, the present model has a wheel force about 40 percent higher than that of the original X-1 model. No attempt was made to evaluate the effect of deflecting the slotted flap on the damping-in-roll coefficients used in these calculations.

The data of figures 19 and 20 indicate that the rolling-moment-coefficient, yawing-moment-coefficient, and lateral-force-coefficient curves were generally linear for angles of sideslip of about  $\pm 10^\circ$ . The data of figure 21 show that the rudder and ailerons were capable of trimming the model through sideslip angles of about  $\pm 10^\circ$  for the flaps-retracted configuration and about  $\pm 8^\circ$  for the flaps-deflected configuration. The original model was able to maintain steady sideslip angles of about  $\pm 8^\circ$ .

The yawing-moment-coefficient and rolling-moment-coefficient data of figures 16, 17, 19, and 20 were assumed to be symmetrical about zero for these calculations.

#### CONCLUSIONS

The results of an investigation to determine the low-speed stability and control characteristics of a  $\frac{1}{4}$ -scale model of the Bell X-1 airplane modified to include a wing of aspect ratio 4, taper ratio 0.5,  $0^\circ$  sweepback

of the 0.40 chord line, and a modified NACA 64A004 airfoil section indicate the following conclusions:

1. The model with flaps at  $0^\circ$  had elevator-fixed static longitudinal stability amounting generally to a static margin of about 0.12 mean aerodynamic chord throughout most of the lift-coefficient range and became extremely stable near the stall. With flaps deflected to  $\delta_f = 35^\circ$  the elevator-fixed static margin was about 0.04 mean aerodynamic chord for most of the lift-coefficient range and became increasingly stable near the stall.
2. The maximum balanced lift coefficient was 0.70 for the flaps-up condition and 1.04 for the flaps-deflected condition. The optimum flap deflection tested for the slotted flap was found to be  $35^\circ$ ; this deflection caused an increment in lift coefficient of 0.64 for an angle of attack of  $4^\circ$ .
3. The model possessed static directional stability through the range investigated and this stability was generally unaffected by deflecting the slotted flap. The effective dihedral was positive and generally constant throughout the angle-of-attack range and was only slightly affected by deflecting the slotted flaps.
4. The effectiveness of the rudder through the deflection range investigated ( $\pm 15^\circ$ ) was adequate to trim the model through a sideslip range of  $\pm 10^\circ$  flaps retracted and  $\pm 8^\circ$  for flaps deflected  $35^\circ$ .
5. The aileron effectiveness was satisfactory through the stall for both the flaps-retracted and flaps-deflected conditions although a loss in effectiveness was present near the stall.

Langley Aeronautical Laboratory,  
National Advisory Committee for Aeronautics,  
Langley Field, Va., August 18, 1953.

## REFERENCES

1. Gillis, Clarence L., Polhamus, Edward C., and Gray, Joseph L., Jr.: Charts for Determining Jet-Boundary Corrections for Complete Models in 7- by 10-Foot Closed Rectangular Wind Tunnels. NACA WR L-123, 1945. (Formerly NACA ARR L5G31)
2. Herriot, John G.: Blockage Corrections for Three-Dimensional-Flow Closed Throat Wind Tunnels, With Consideration of the Effect of Compressibility. NACA Rep. 995, 1950. (Supersedes NACA RM A7B28.)
3. DeYoung, John: Theoretical Additional Span Loading Characteristics of Wings With Arbitrary Sweep, Aspect Ratio, and Taper Ratio. NACA TN 1491, 1947.
4. Lowry, John G., and Schneiter, Leslie E.: Estimation of Effectiveness of Flap-Type Controls on Sweptback Wings. NACA TN 1674, 1948.
5. Langley Research Staff (Compiled by Thomas A. Toll): Summary of Lateral-Control Research. NACA Rep. 868, 1947. (Supersedes NACA TN 1245.)

TABLE I.- FLIGHT CONDITIONS INVESTIGATED

	Condition I	Condition II
Flap deflection, $\delta_f$ , deg	0	35
Weight, lb	13,488	7000
Lift coefficient, $C_L$	0.70	1.03
Altitude, ft	0	0
Velocity, mph	240	143
Dynamic pressure, lb/ft <sup>2</sup>	148	52.5
Mach number	0.32	0.19



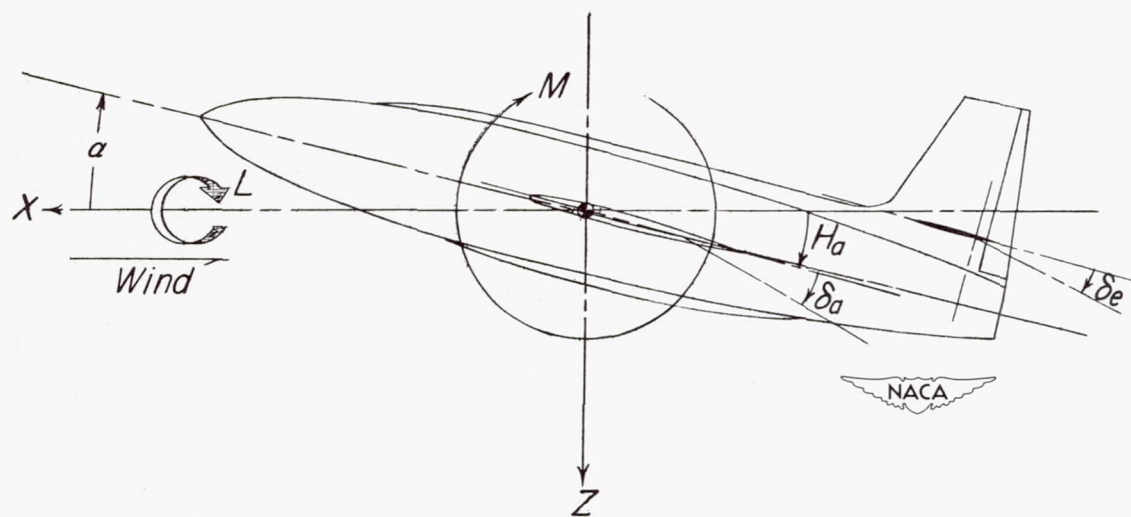
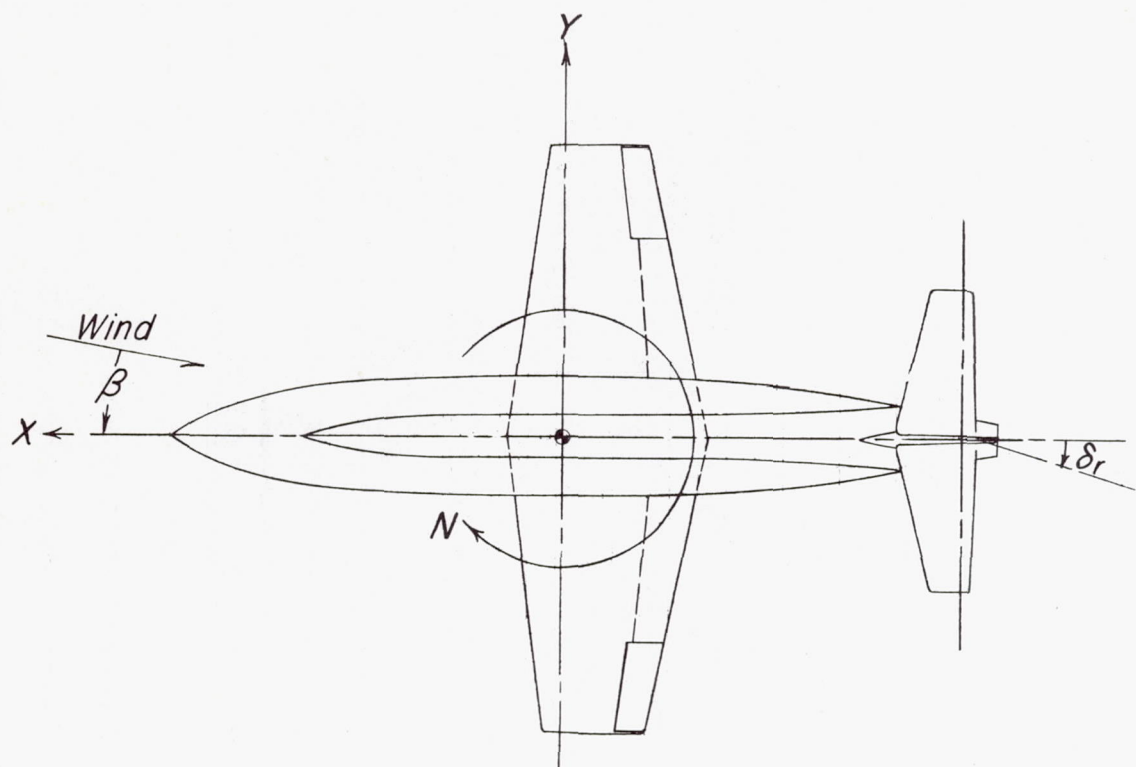
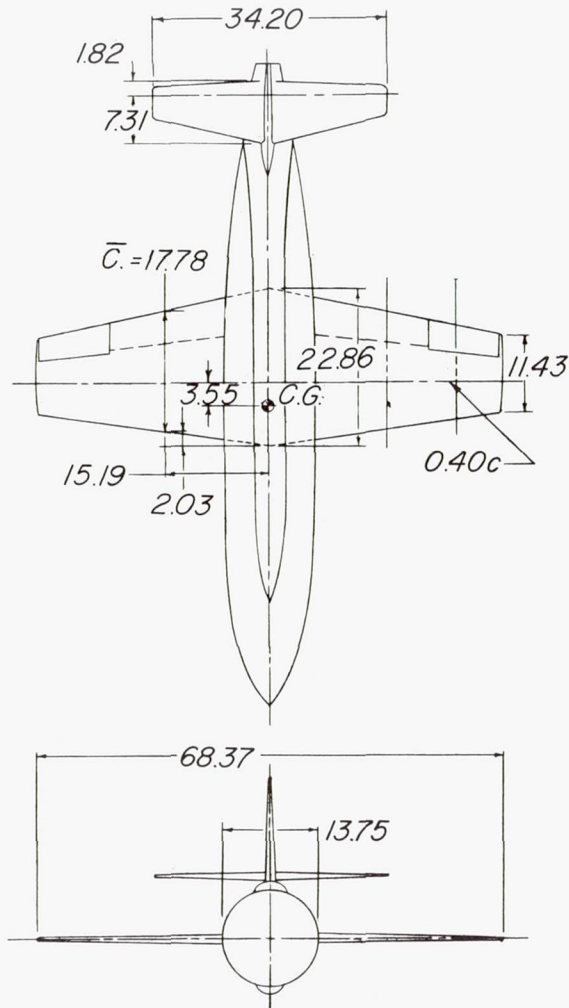


Figure 1.- System of axes showing forces, moments, and angles. Positive values indicated by arrow heads.



(a) Bell X-1 airplane with a thin aspect-ratio-4 wing.

Figure 2.- Three-view drawings of the  $\frac{1}{4}$  - scale models of the Bell X-1 airplane. All dimensions are in inches unless otherwise noted.

## TABULATED DATA

## Wing

Area, total	8.125 sq ft
Area, aileron	0.476 sq ft
Area, slotted flap	1.104 sq ft
Span	5.69 ft
Mean aerodynamic chord	1.48 ft
Aspect ratio	4
Airfoil section	Modified NACA64A004

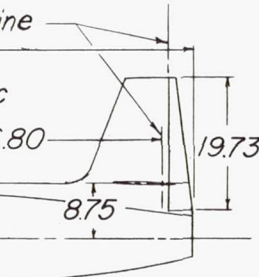
## Horizontal tail

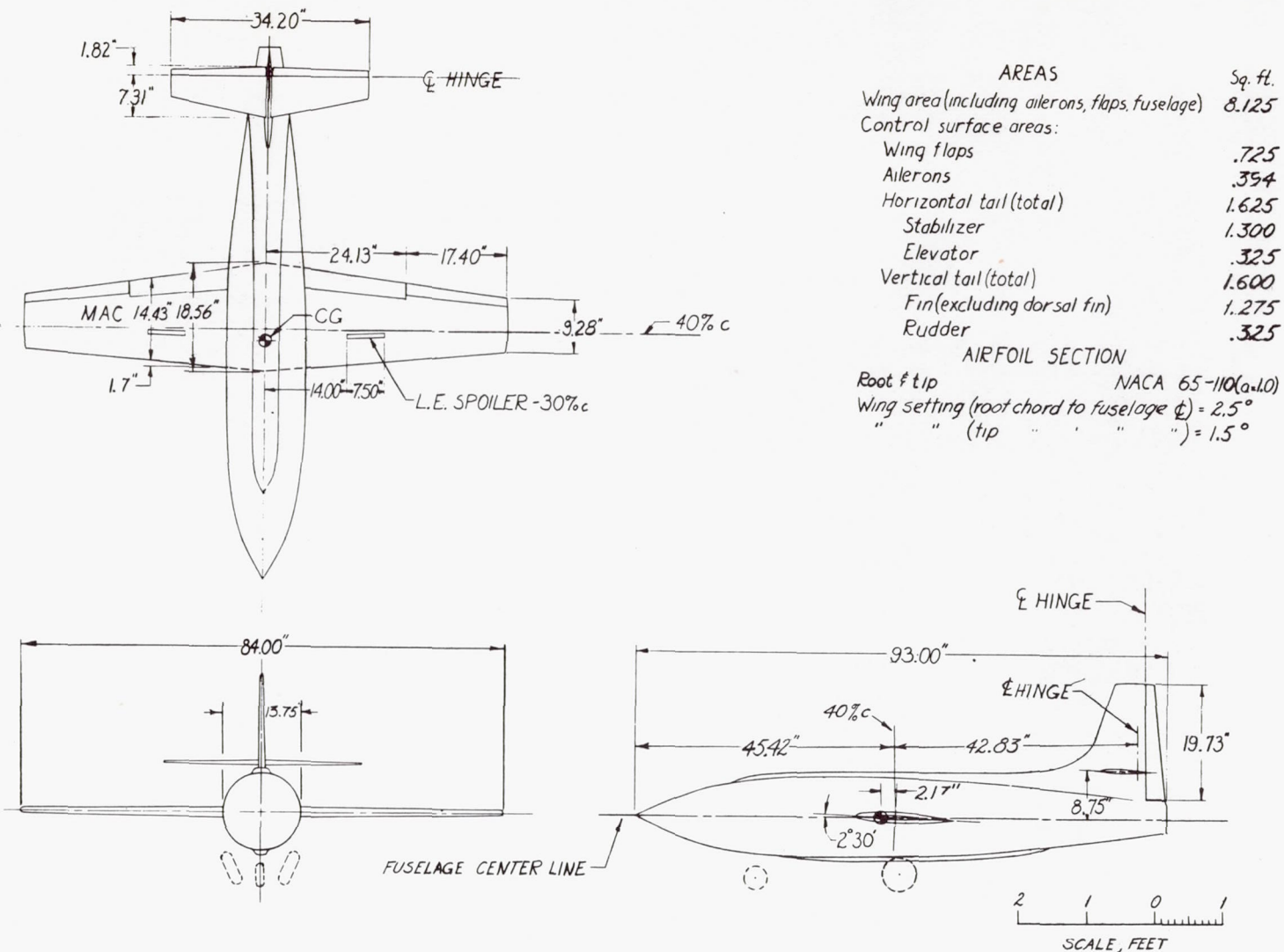
Area, total	1.625 sq ft
Area, elevator	0.325 sq ft
Airfoil section	NACA 65-008



## Vertical tail

Area, total	1.600 sq ft
Area, rudder	0.325 sq ft
Airfoil section	NACA 65-008

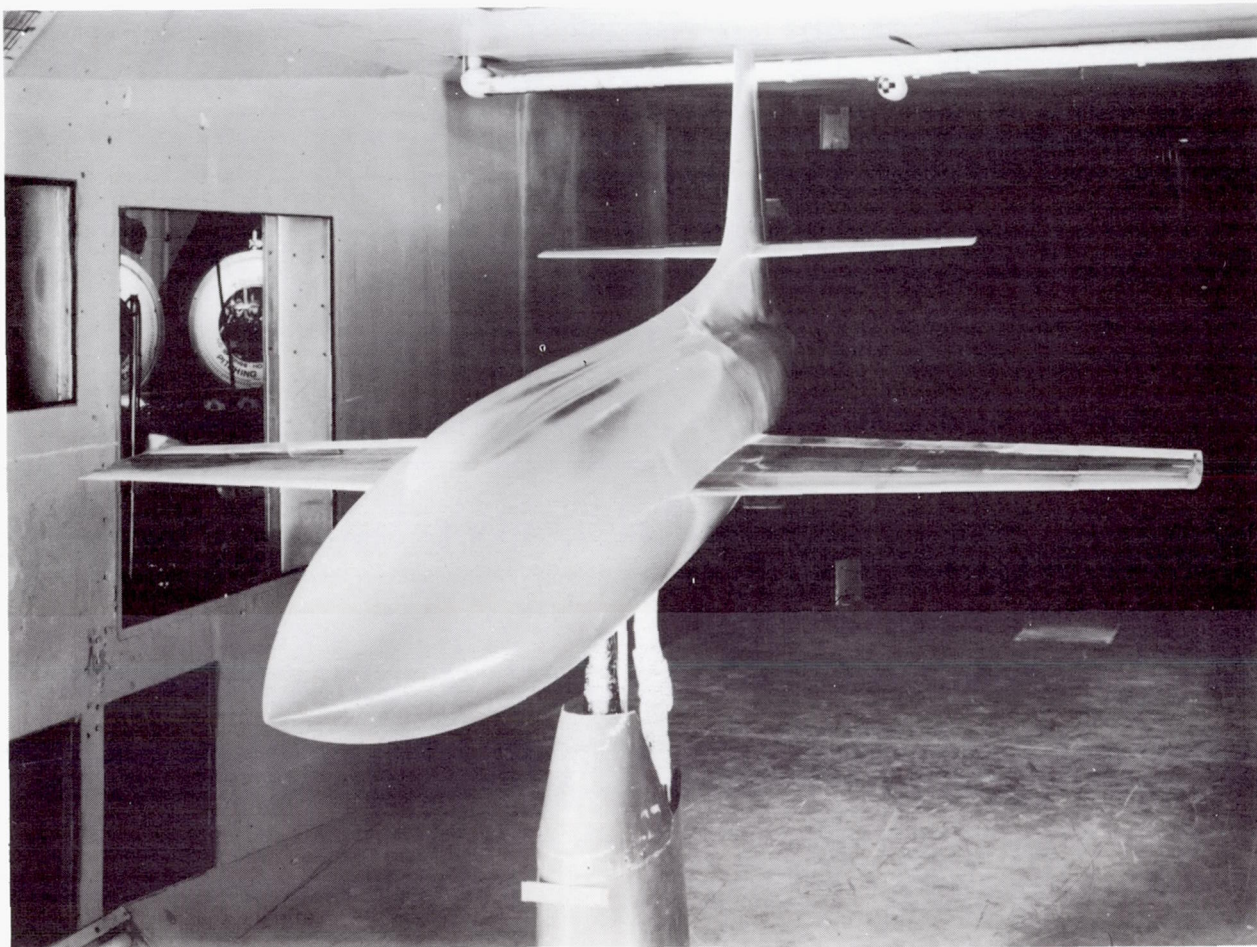




(b) Original Bell X-1 airplane.

Figure 2.- Concluded.

CONFIDENTIAL



L-78613

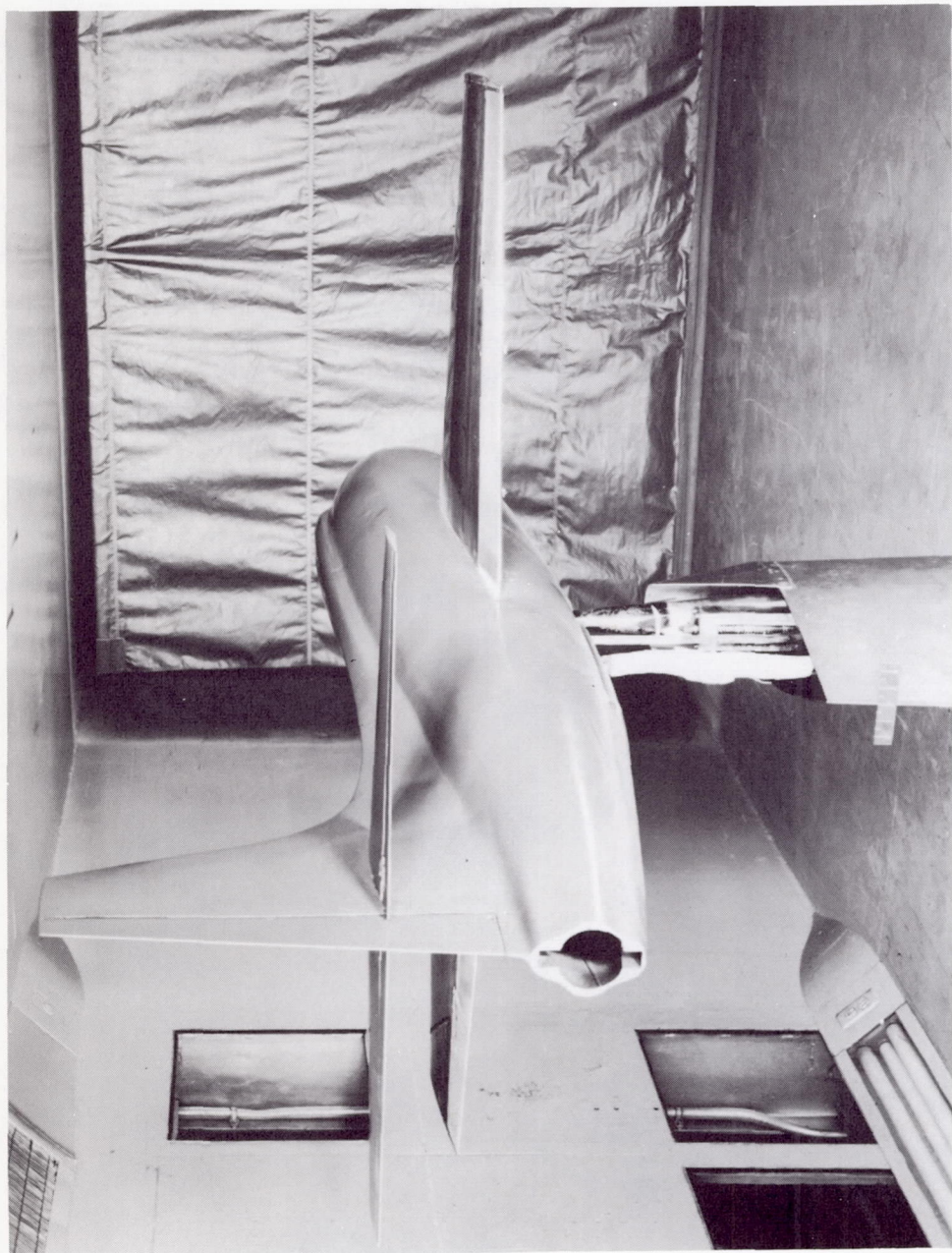
(a) Three-quarter front view,  $\delta_f = 0^\circ$ .

Figure 3.- Views of the model mounted in the 300 MPH 7- by 10-foot tunnel.

CONFIDENTIAL

NACA RM 153H27

16



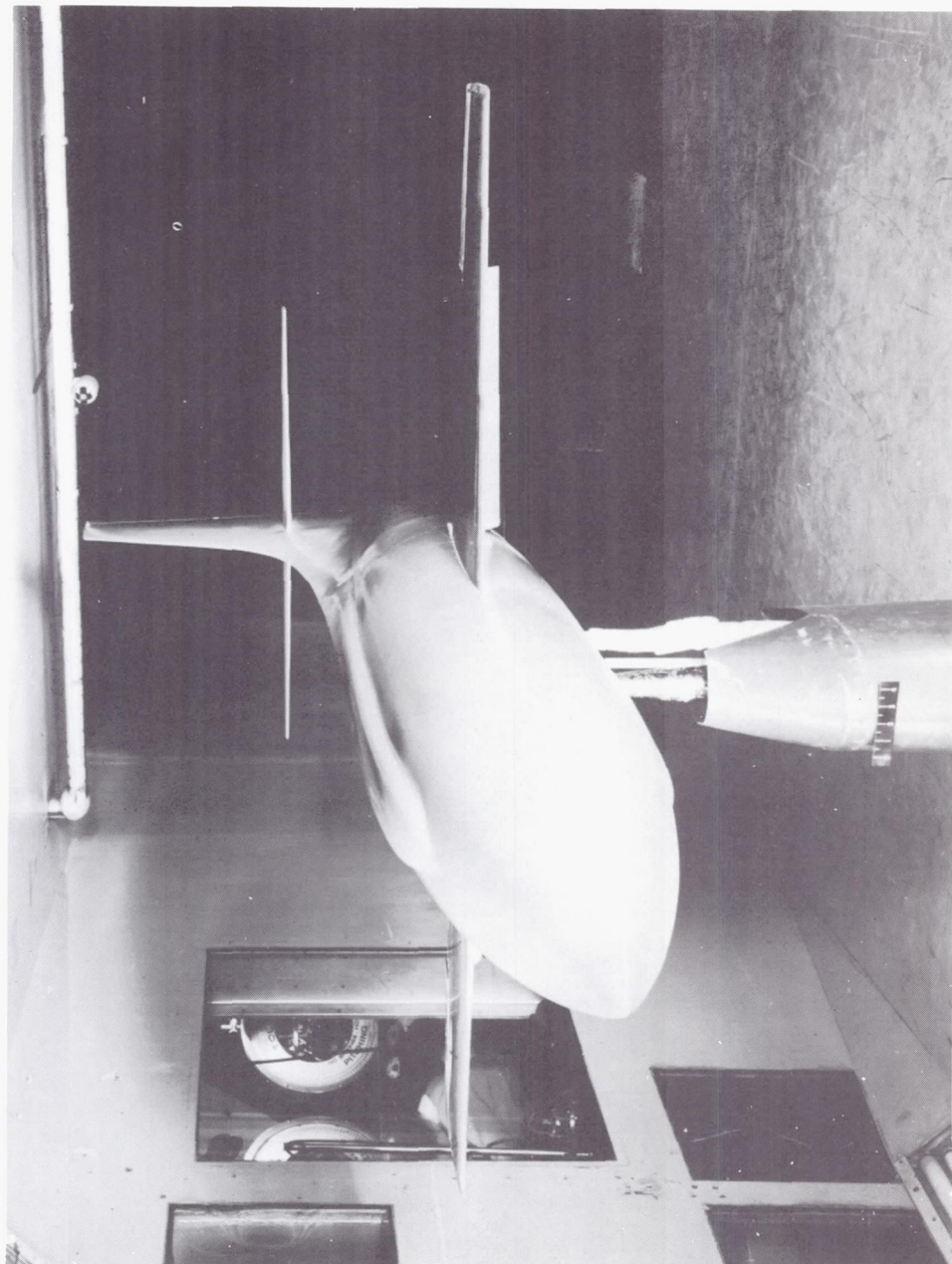
(b) Three-quarter rear view,  $\delta_T = 0^\circ$ .

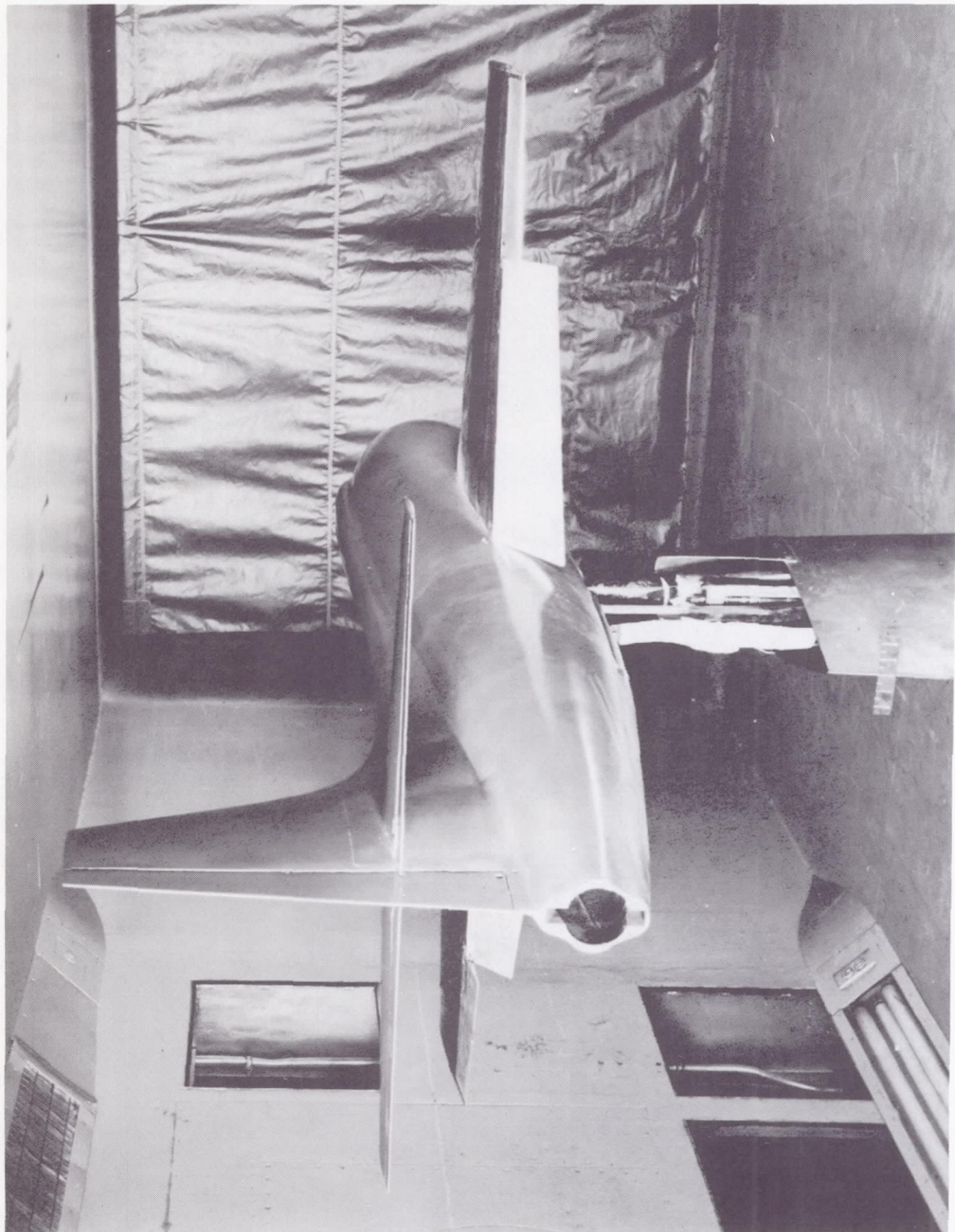
Figure 3.- Continued.

L-78614

(c) Three-quarter front view,  $\delta_f = 35^\circ$ .

Figure 3.- Continued.

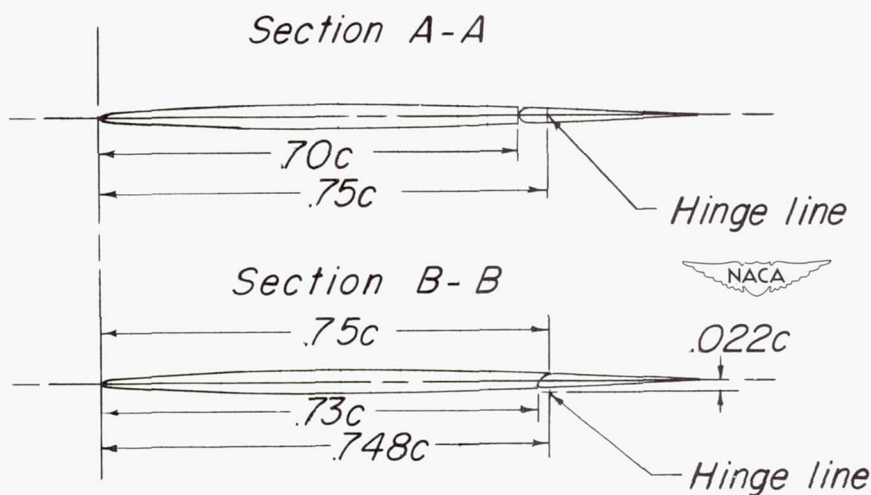
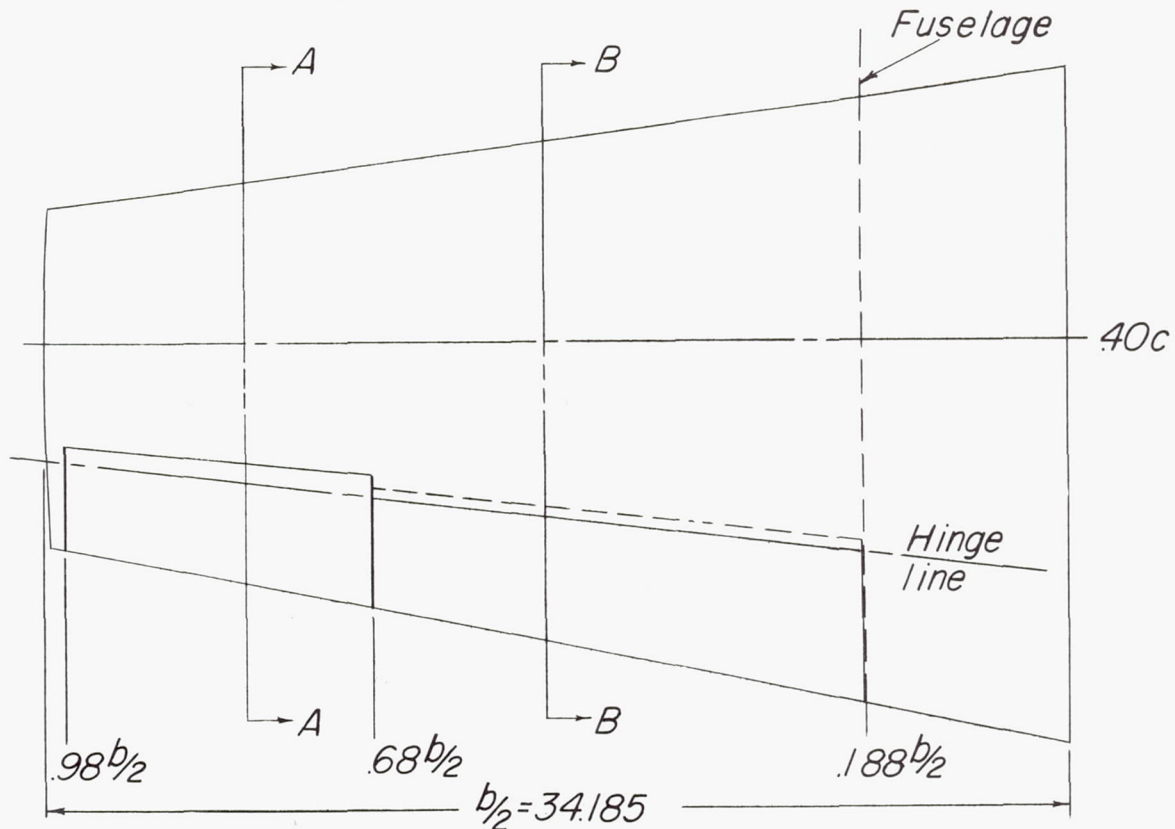




L-78616

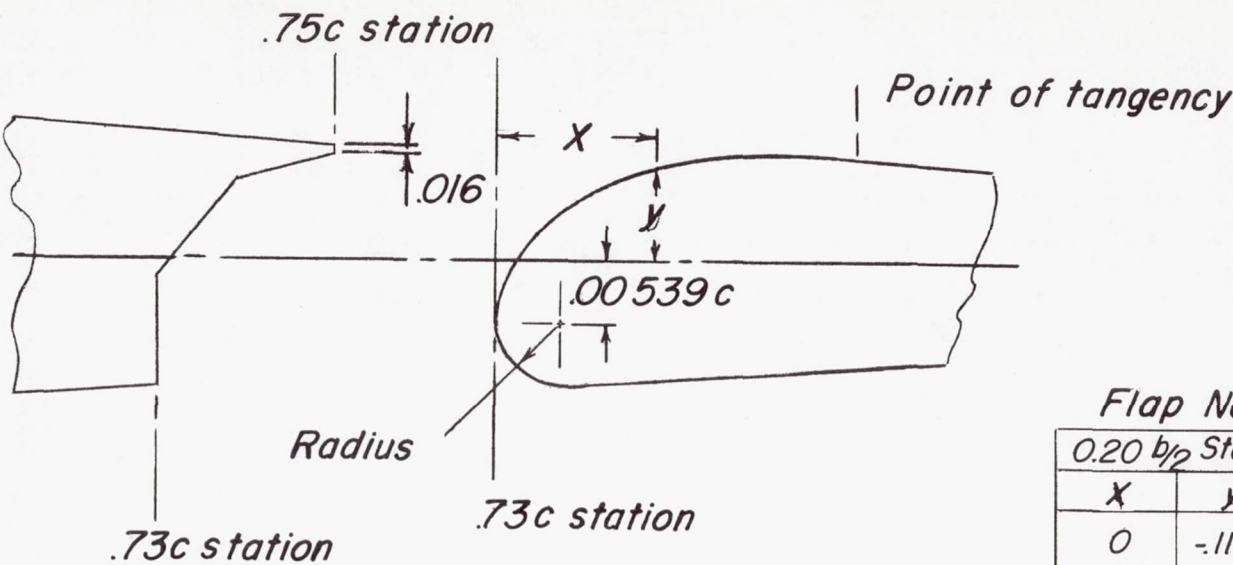
(d) Three-quarter rear view,  $\delta_F = 35^\circ$ .

Figure 3.- Concluded.



(a) General arrangement.

Figure 4.- Details of flaps and ailerons tested.



Flap Nose Ordinates

0.20 $b/2$ Sta.		0.68 $b/2$ Sta.	
$x$	$y$	$x$	$y$
0	-.111	0	-.081
.006	-.061	.002	-.056
.026	-.011	.010	-.031
.061	.039	.040	.019
.114	.089	.096	.069
.194	.139	.196	.119
.251	.164	.261	.138
.329	.189	.298	.146
.373	.199	.336	.152
.448	.211	.398	.157
.548	.216	.436	.158
.578	.214	.486	.157
5.563	.031	4.074	.031



(b) Flap-nose shape.

Figure 4.- Concluded.

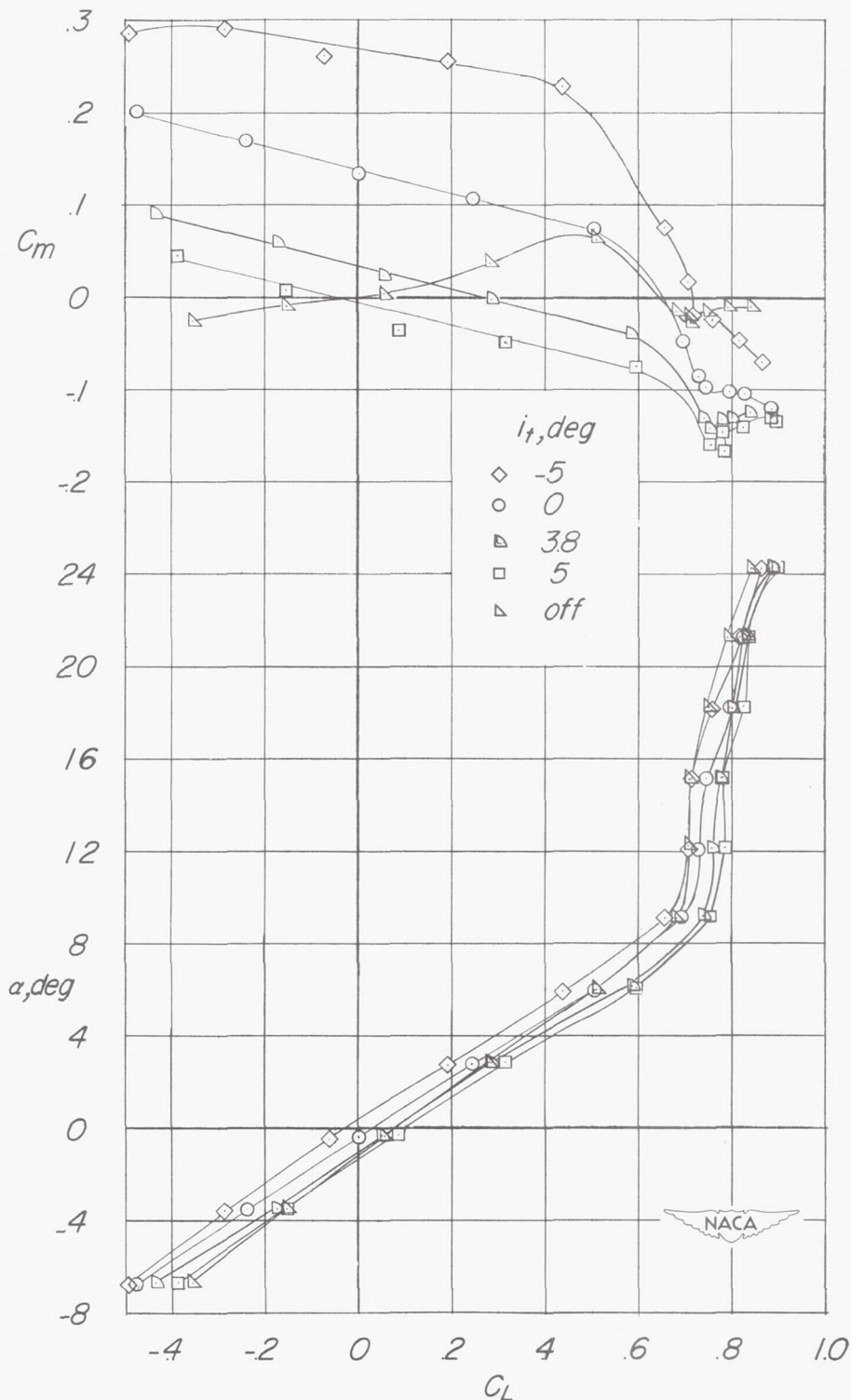


Figure 5.- Effect of stabilizer setting on the aerodynamic characteristics in pitch of a 1/4-scale model of the Bell X-1 airplane equipped with a 4-percent-thick, aspect-ratio-4 wing.  $\delta_f = 0^\circ$ ;  $\delta_a = 0^\circ$ ;  $\delta_r = 0^\circ$ ;  $\delta_e = 0^\circ$ ;  $\beta = 0^\circ$ .

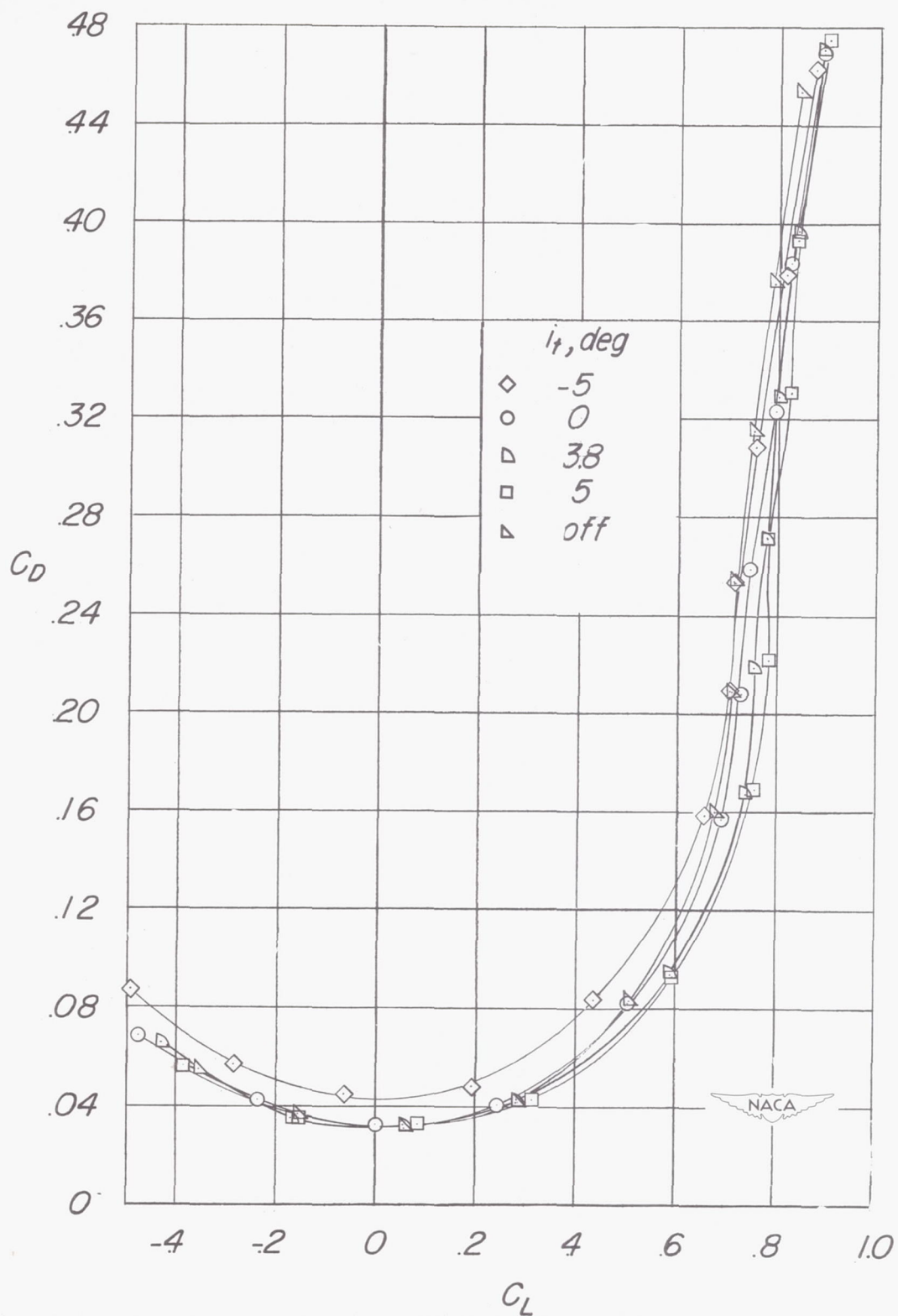


Figure 5.- Concluded.

.3

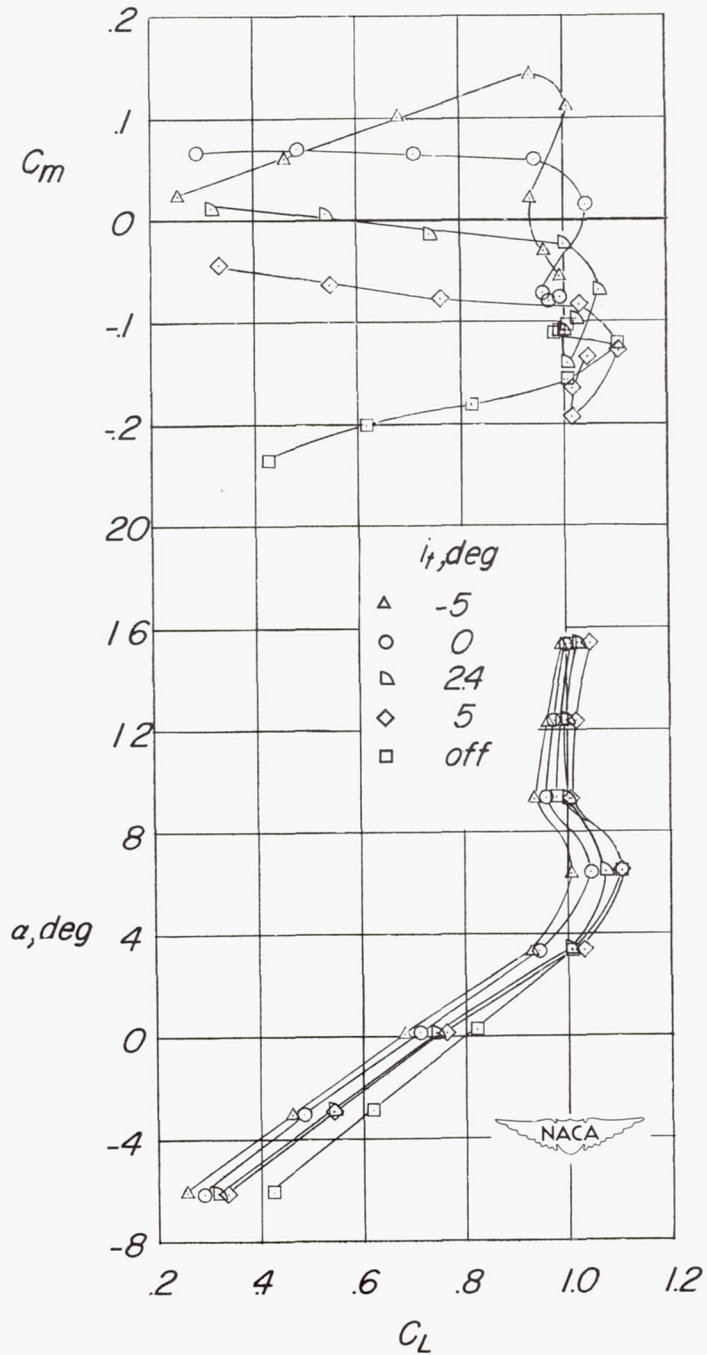


Figure 6.- Effect of stabilizer setting on the aerodynamic characteristics in pitch of a 1/4-scale model of the Bell X-1 airplane equipped with a 4-percent-thick, aspect-ratio-4 wing.  $\delta_f = 35^\circ$ ;  $\delta_a = 0^\circ$ ;  $\delta_r = 0^\circ$ ;  $\delta_e = 0^\circ$ ;  $\beta = 0^\circ$ .

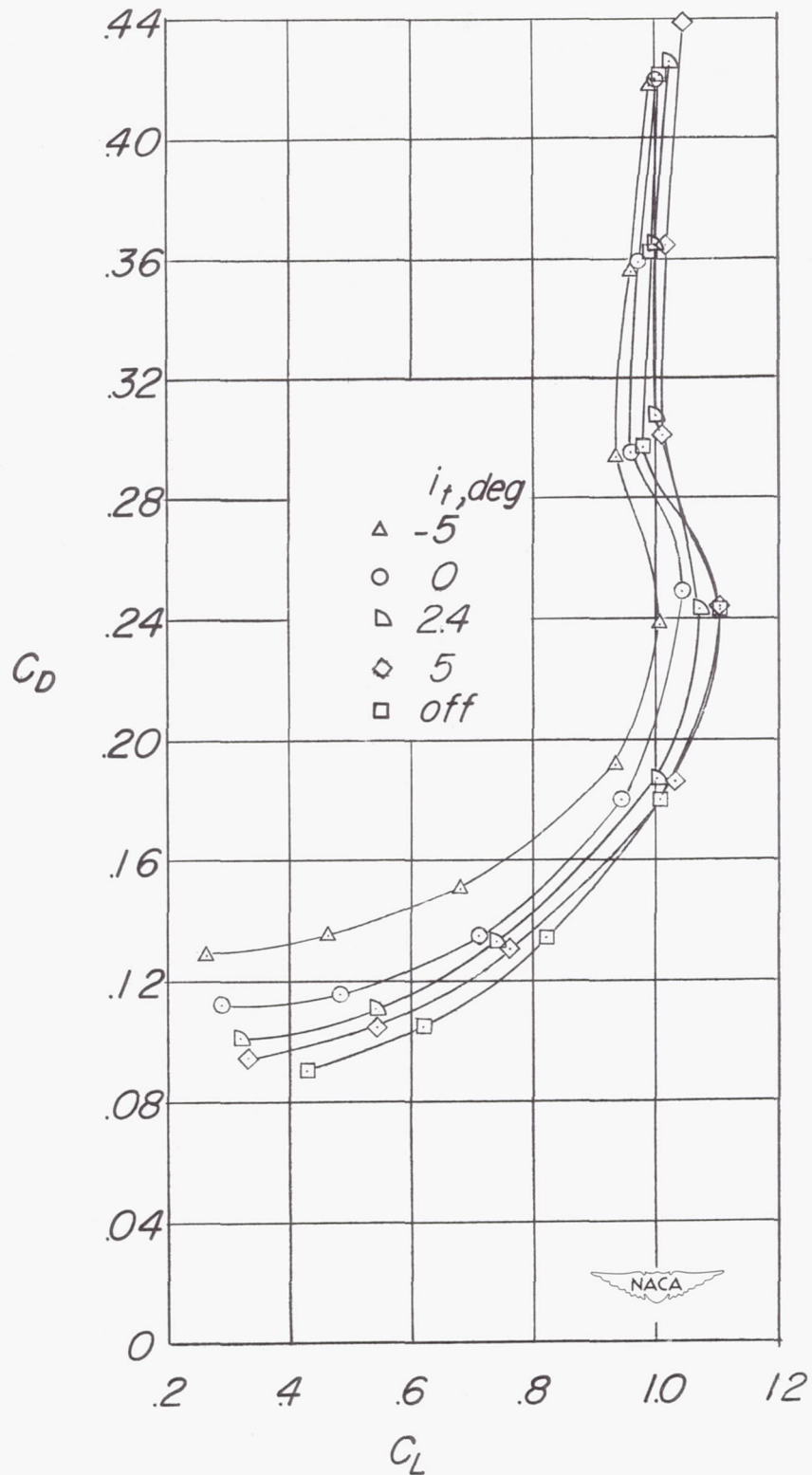


Figure 6.- Concluded.

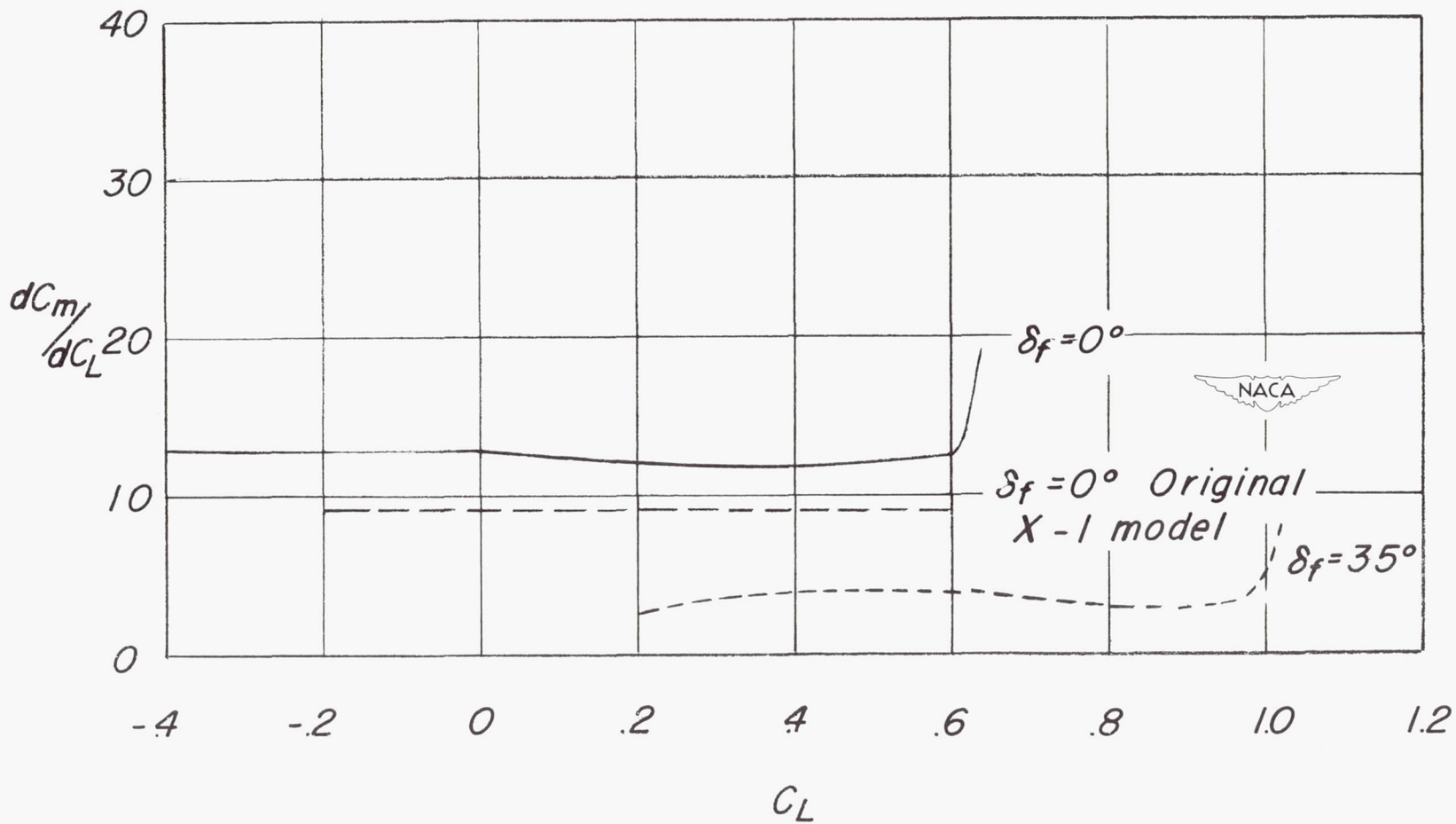
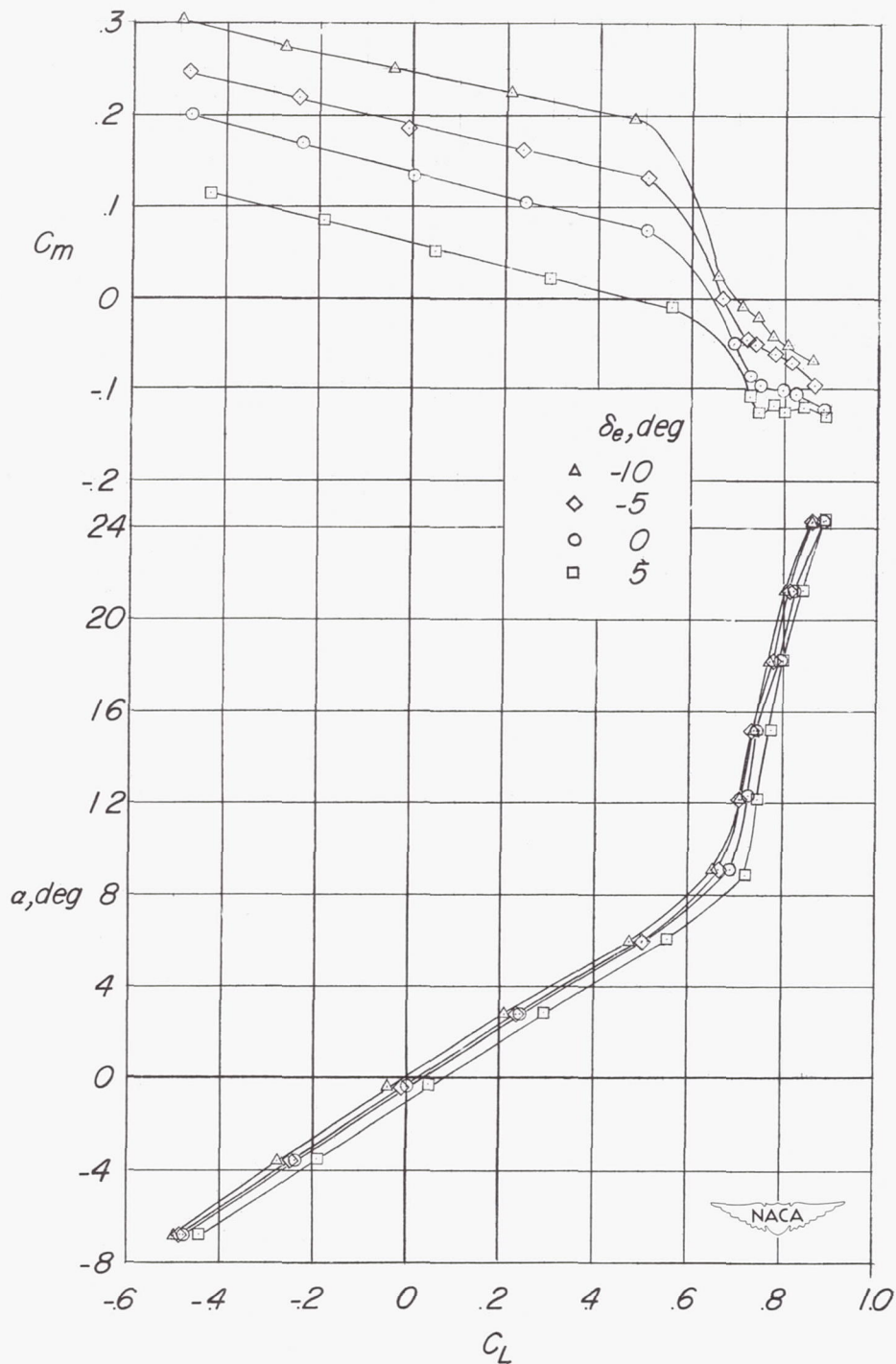
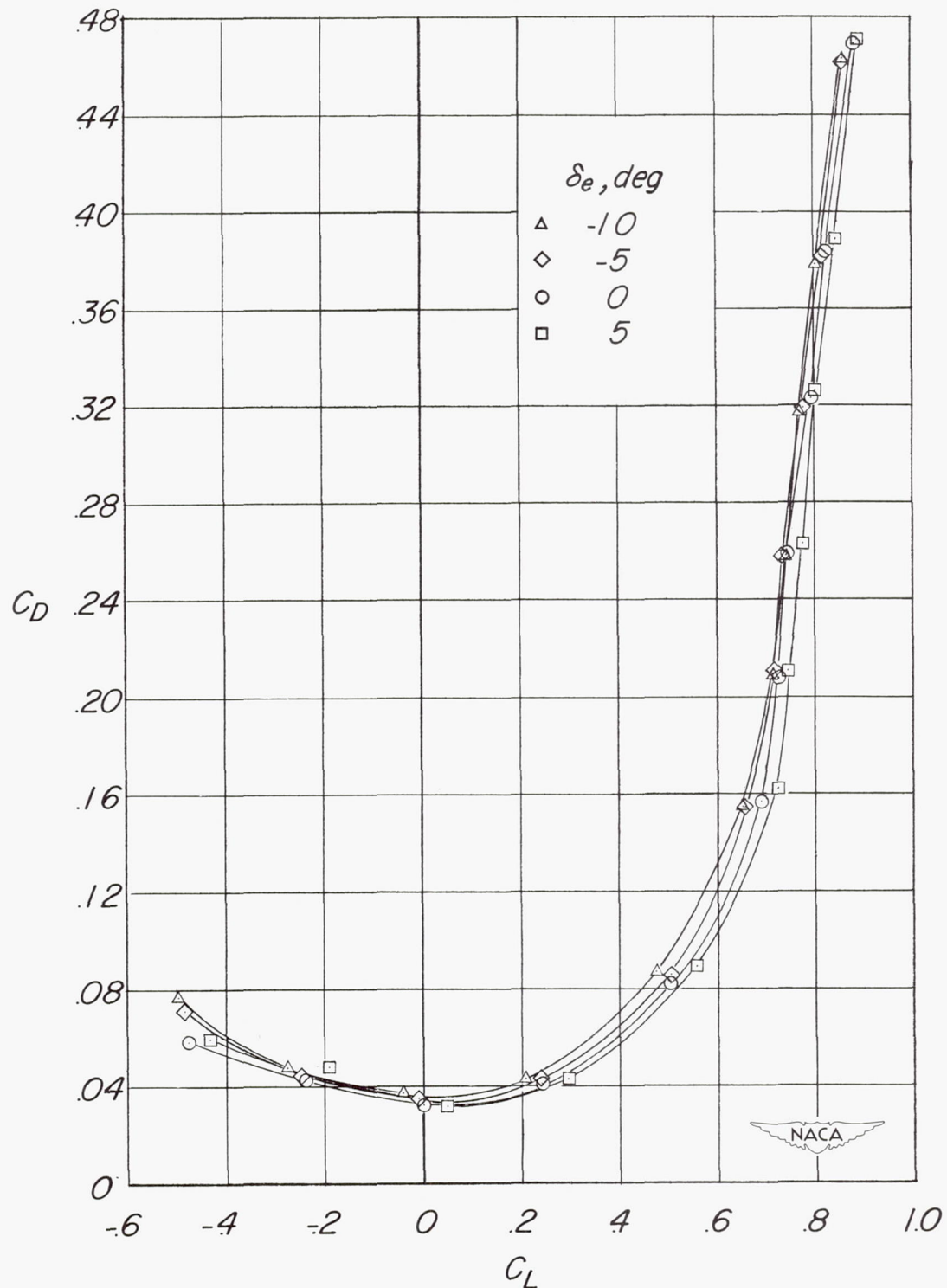


Figure 7.- Variation of static margin with lift coefficient for the 1/4-scale Bell X-1 airplane.  $i_t = 0^\circ$ .



(a)  $i_t = 0^\circ$ .

Figure 8.- Effect of elevator deflection on the aerodynamic characteristics in pitch of a 1/4-scale model of the Bell X-1 airplane equipped with a 4-percent-thick, aspect-ratio-4 wing.  $\delta_f = 0^\circ$ ;  $\delta_a = 0^\circ$ ;  $\delta_r = 0^\circ$ ;  $\beta = 0^\circ$ .



(a) Concluded.

Figure 8.- Continued.

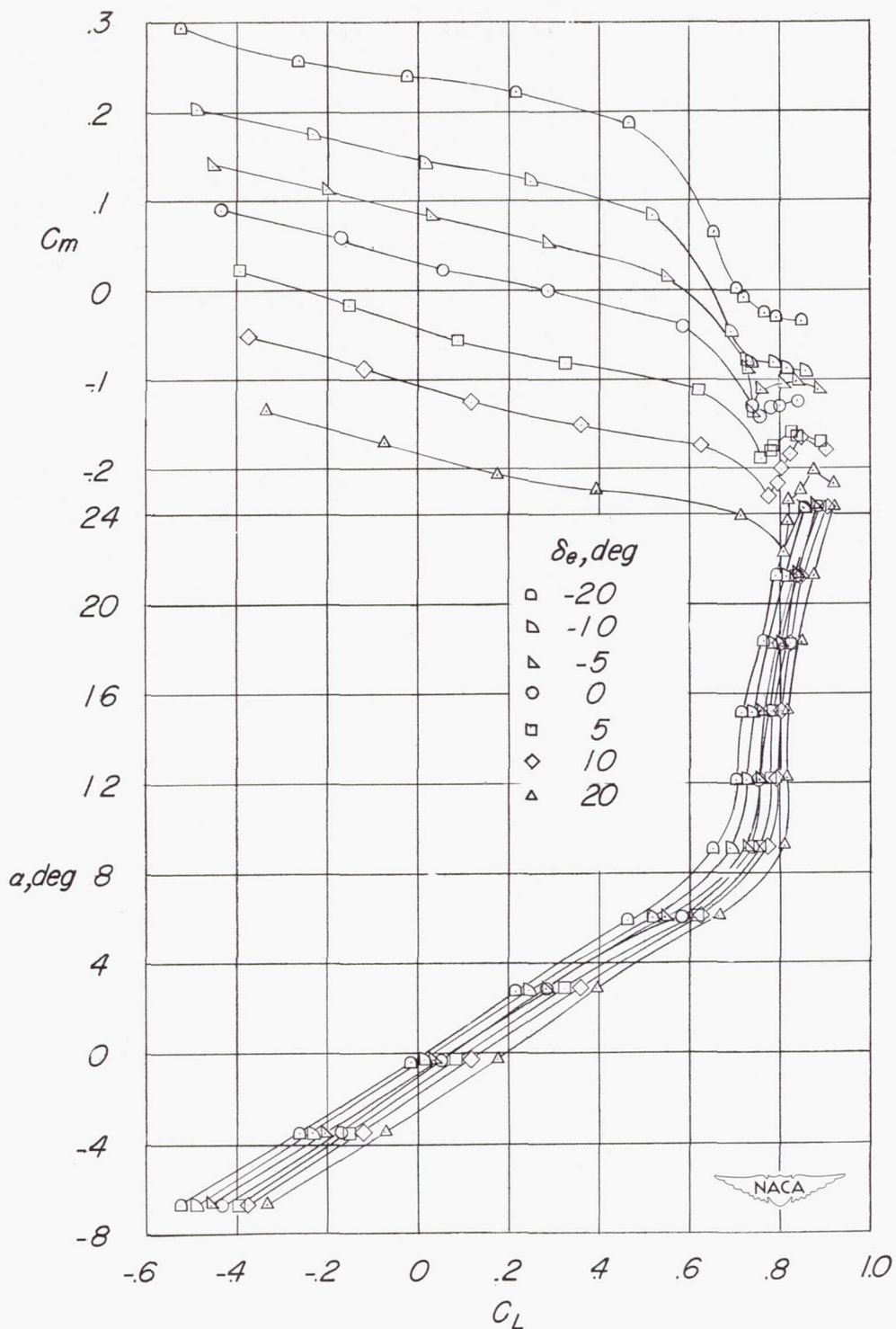
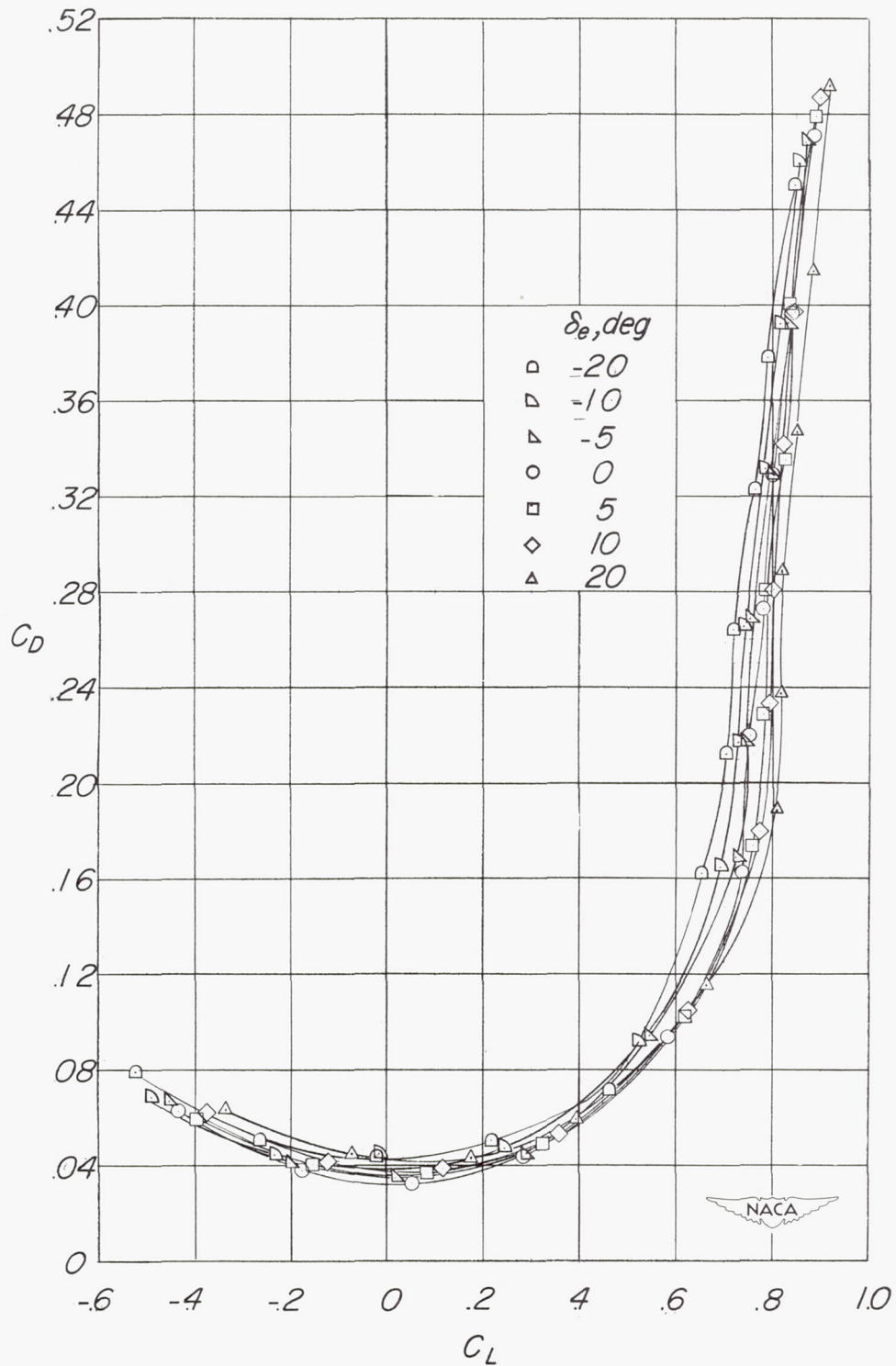
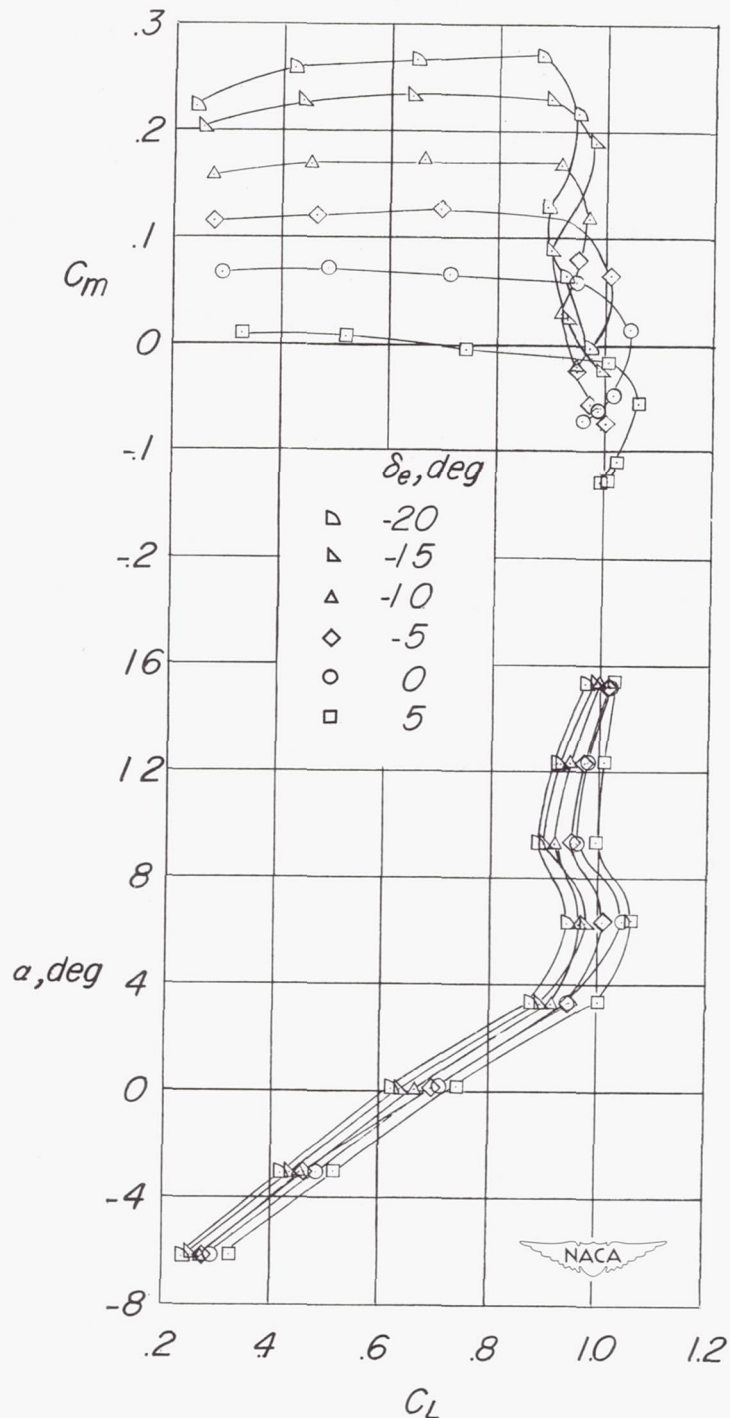
(b)  $it = 38^\circ$ .

Figure 8.- Continued.



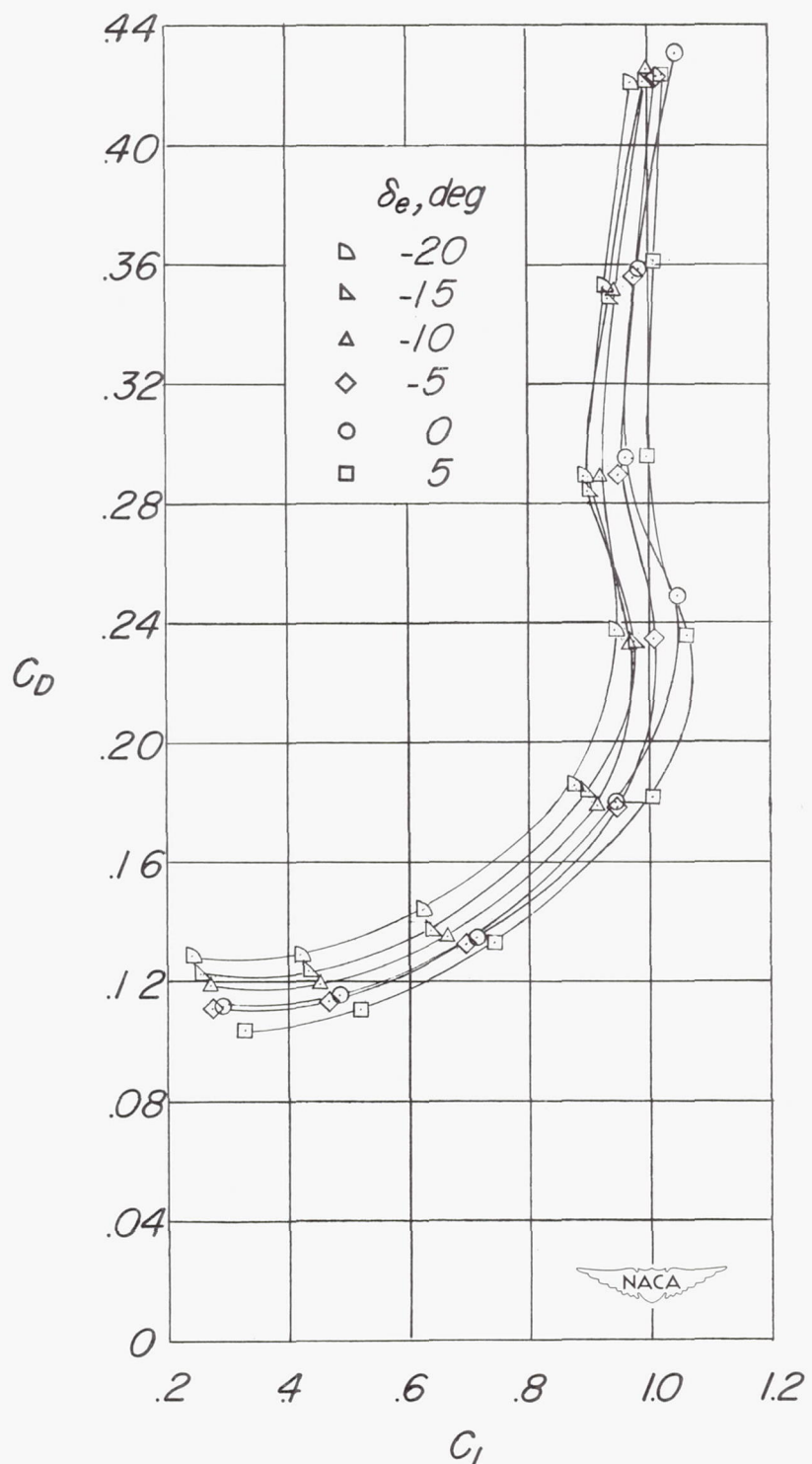
(b) Concluded.

Figure 8.- Concluded.



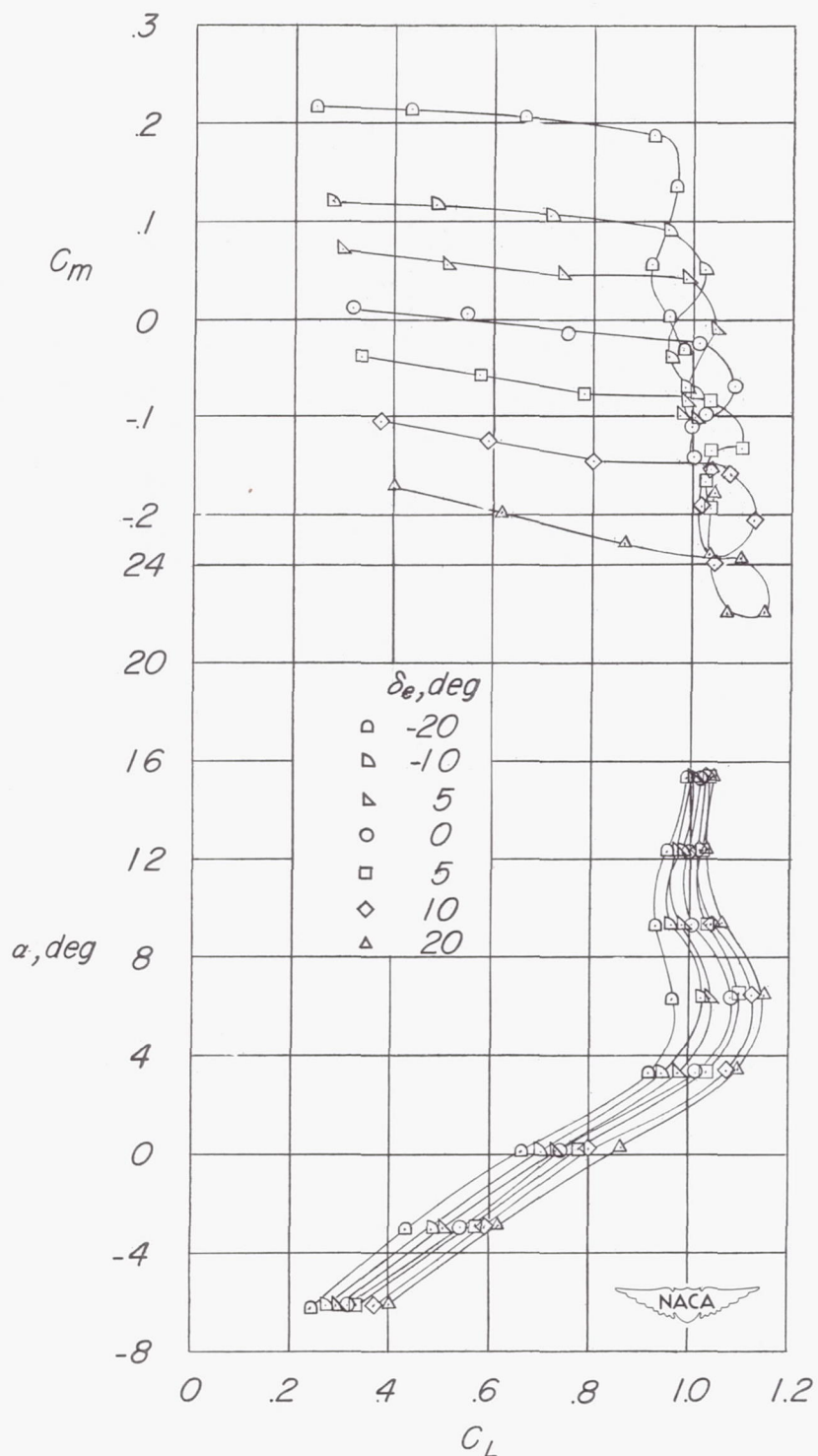
(a)  $i_t = 0^\circ$ .

Figure 9.- Effect of elevator deflection on the aerodynamic characteristics in pitch of a 1/4-scale model of the Bell X-1 airplane equipped with a 4-percent-thick, aspect-ratio-4 wing.  $\delta_f = 35^\circ$ ;  $\delta_a = 0^\circ$ ;  $\delta_r = 0^\circ$ ;  $\beta = 0^\circ$ .



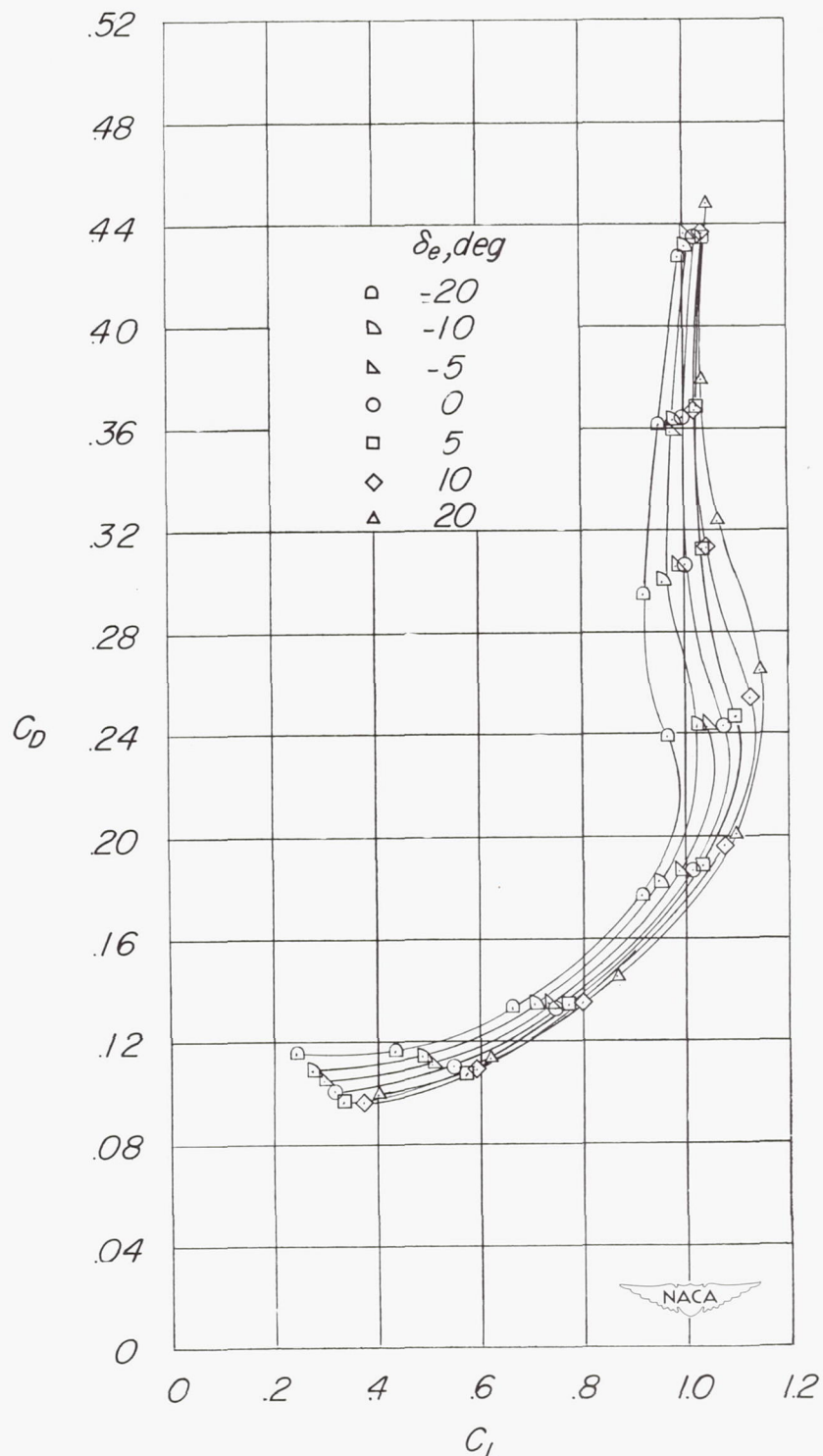
(a) Concluded.

Figure 9.- Continued.



(b)  $i_t = 2.4^\circ$ .

Figure 9..- Continued.



(b) Concluded.

Figure 9.- Concluded.

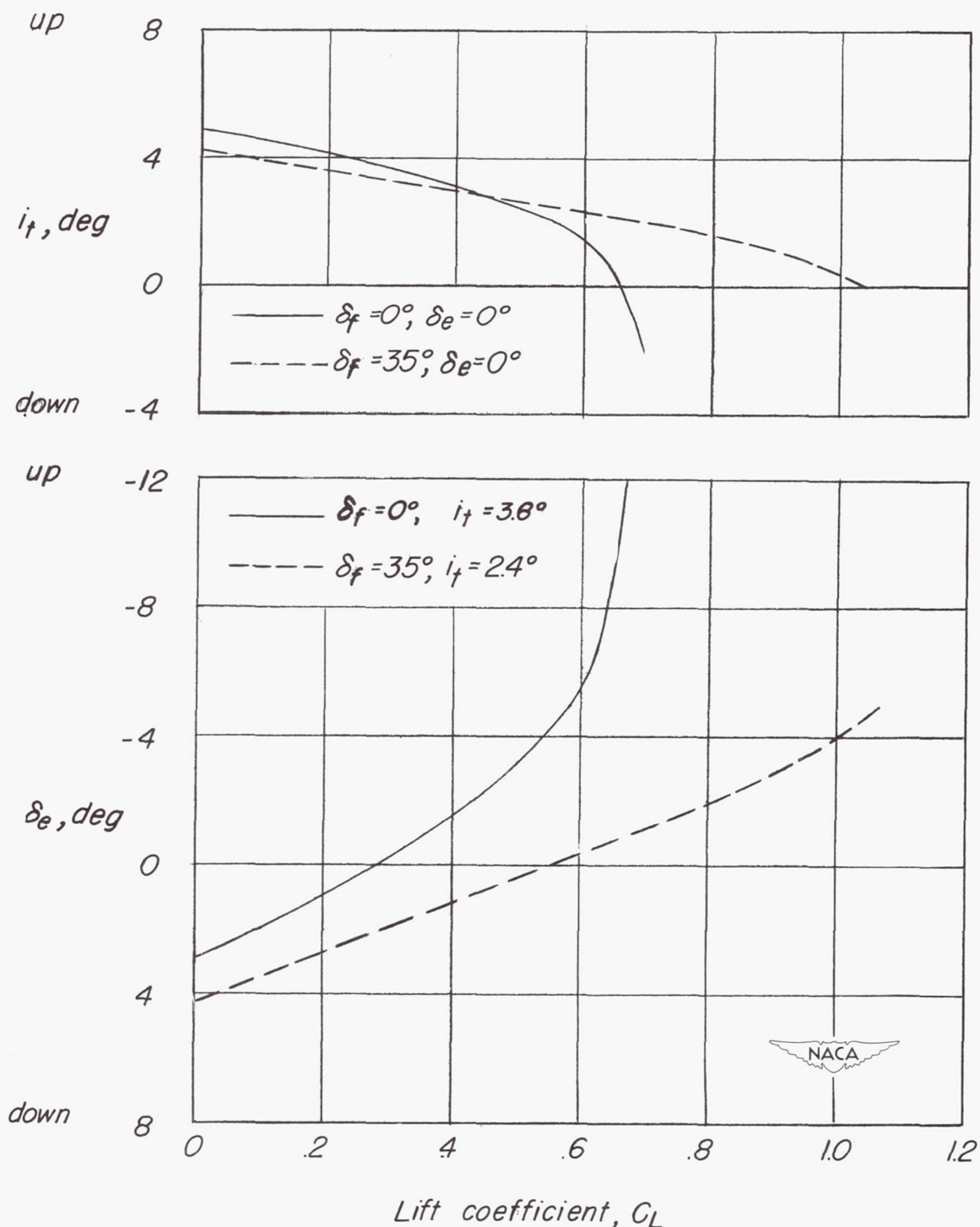


Figure 10.- Elevator deflection and horizontal-tail incidence required to trim through the lift-coefficient range.

.3

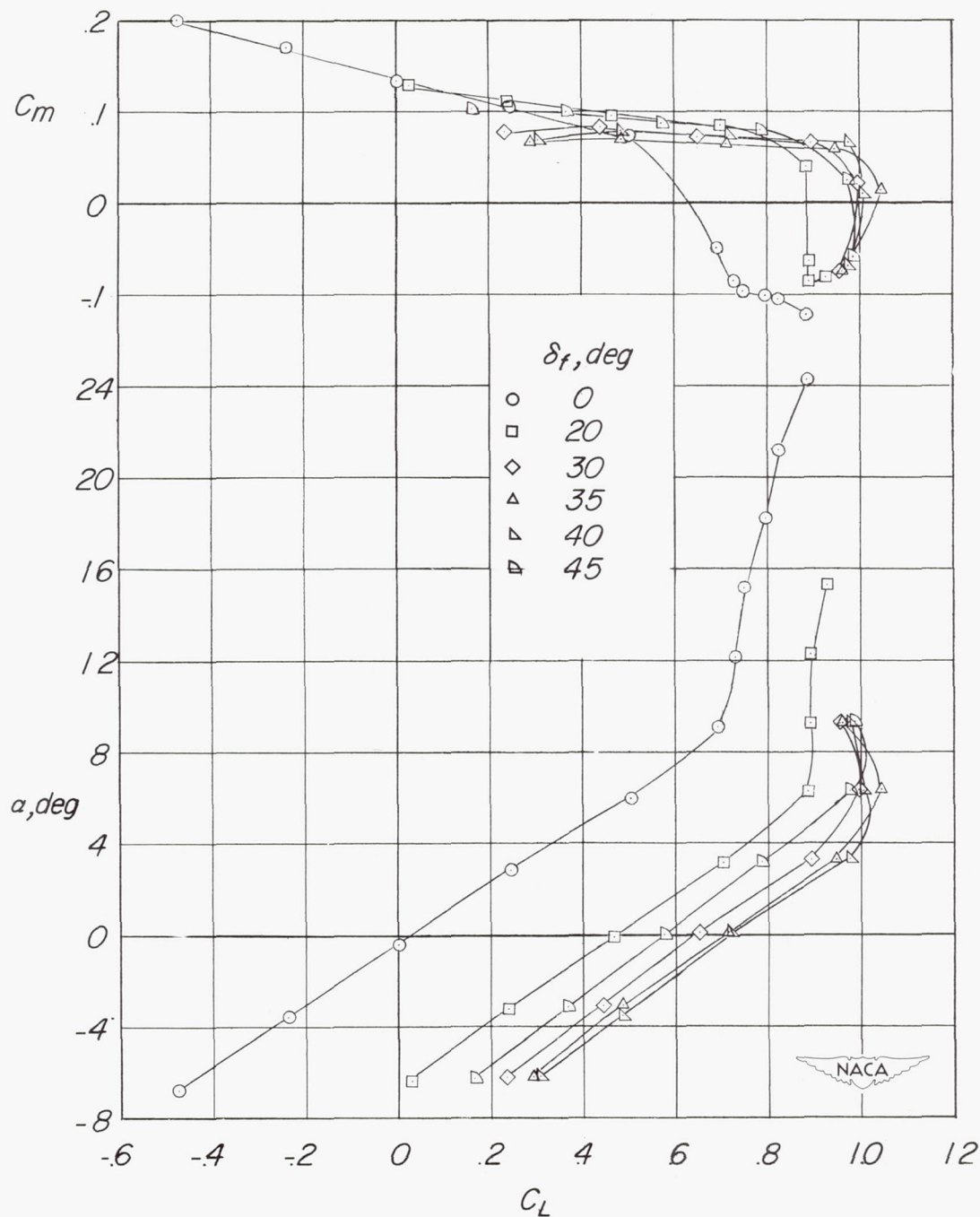


Figure 11.- Effect of flap deflection on the aerodynamic characteristics in pitch of a 1/4-scale model of the Bell X-1 airplane equipped with a 4-percent-thick, aspect-ratio-4 wing.  $\delta_a = 0^\circ$ ;  $\delta_r = 0^\circ$ ;  $\delta_e = 0^\circ$ ;  $i_t = 0^\circ$ ;  $\beta = 0^\circ$ .

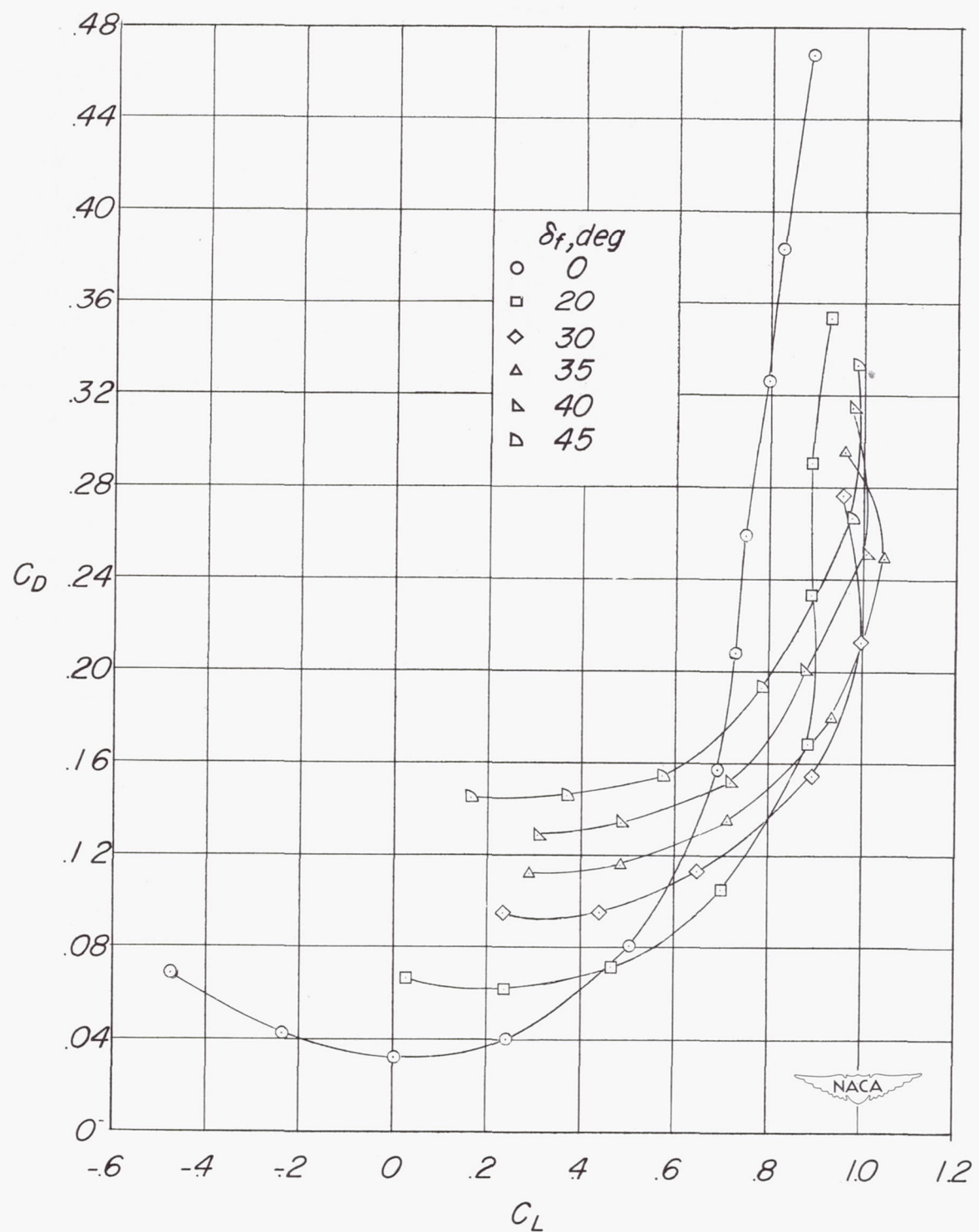


Figure 11.- Concluded.

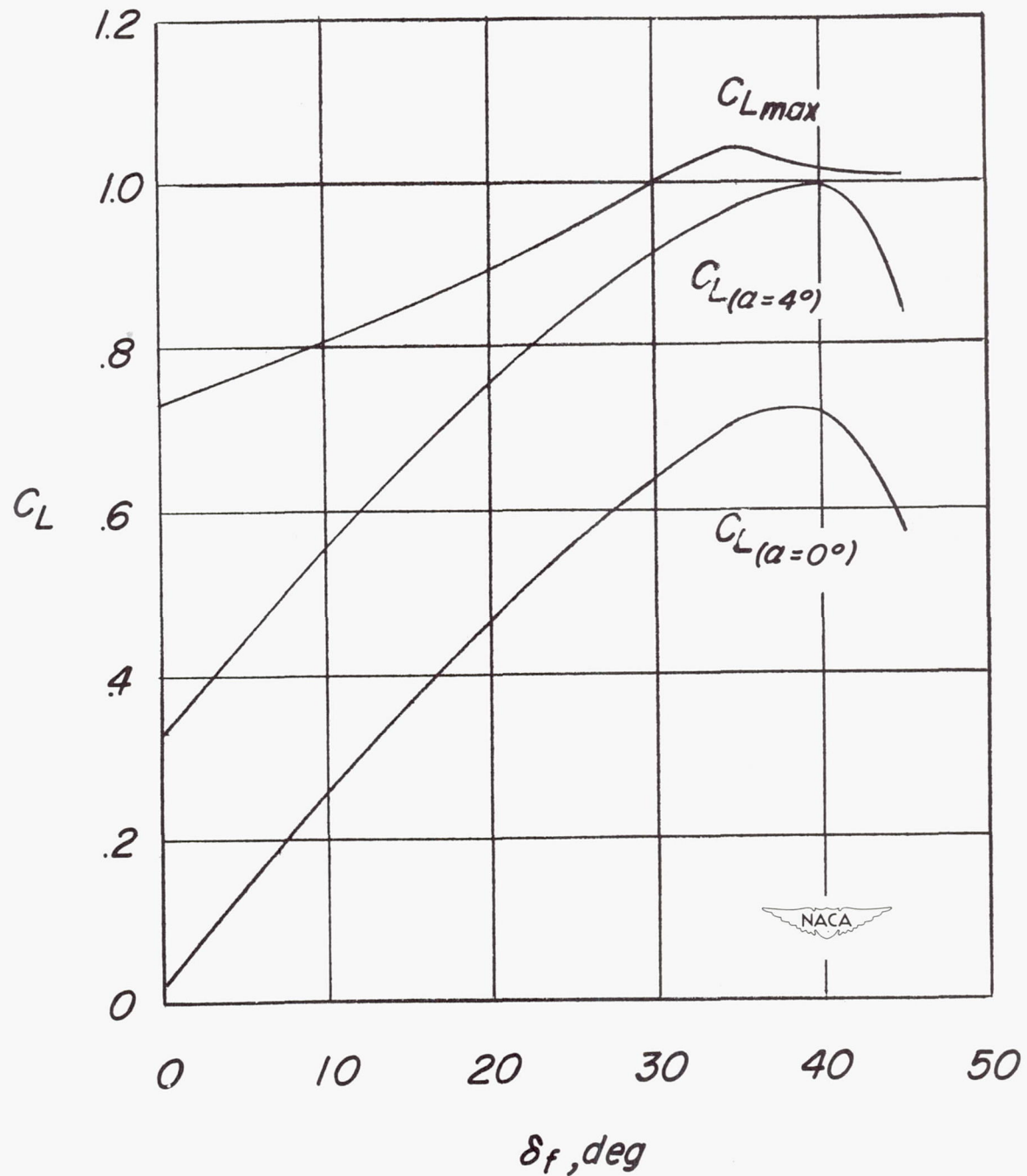


Figure 12.- Variation of lift coefficient with flap deflection for  $\alpha = 0^\circ$ ,  $\alpha = 4^\circ$ , and  $C_{L\max}$ .  $it = 0^\circ$ ;  $\delta_e = 0^\circ$ .

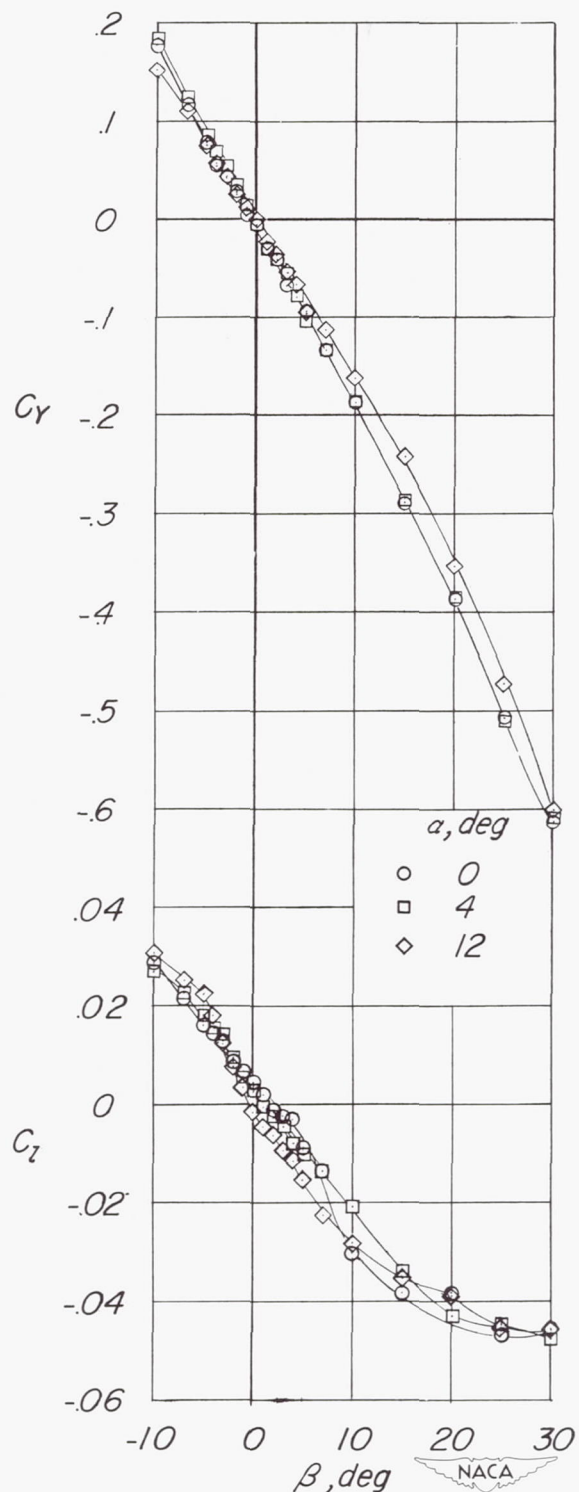


Figure 13.- Effect of angle of attack on the aerodynamic characteristics in sideslip of a 1/4-scale model of the Bell X-1 airplane equipped with a 4-percent-thick, aspect-ratio-4 wing.  $\delta_f = 0^\circ$ .

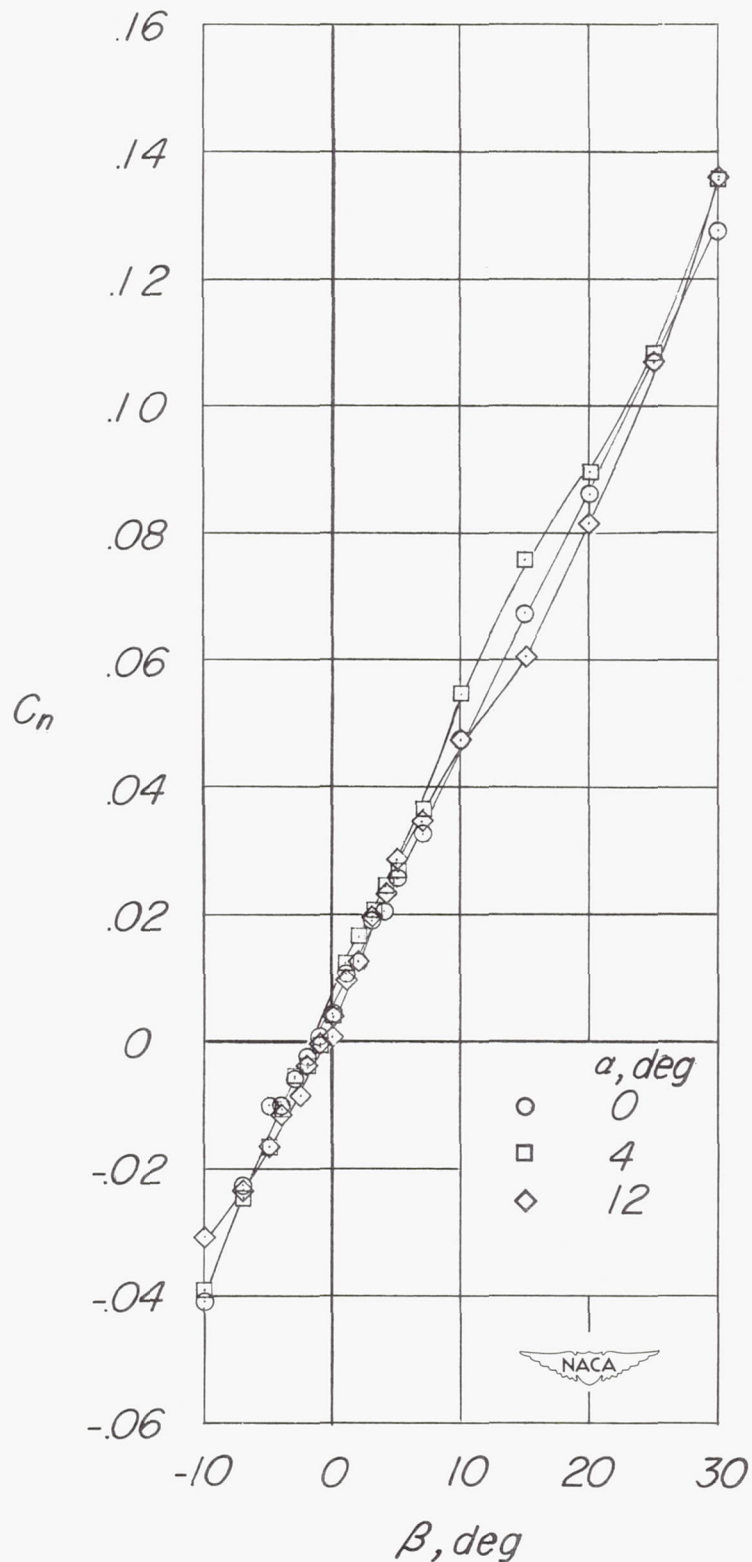


Figure 13.- Concluded.

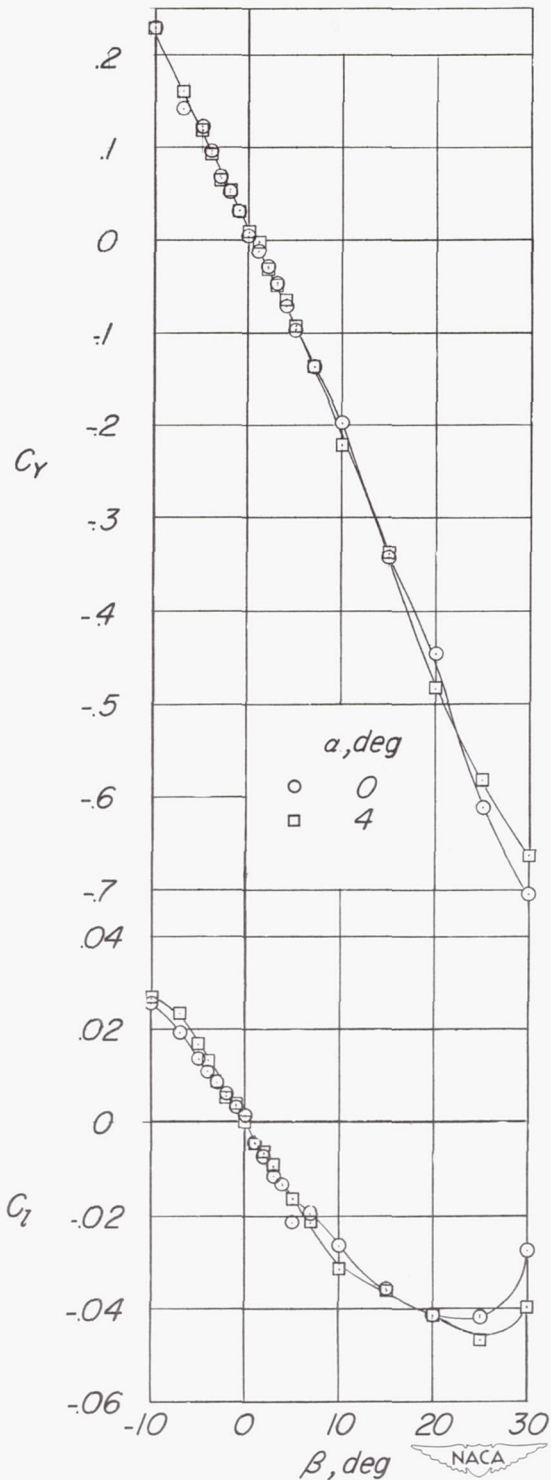


Figure 14.- Effect of angle of attack on the aerodynamic characteristics in sideslip of a 1/4-scale model of the Bell X-1 airplane equipped with a 4-percent-thick, aspect-ratio-4 wing.  $\delta_f = 35^\circ$ .

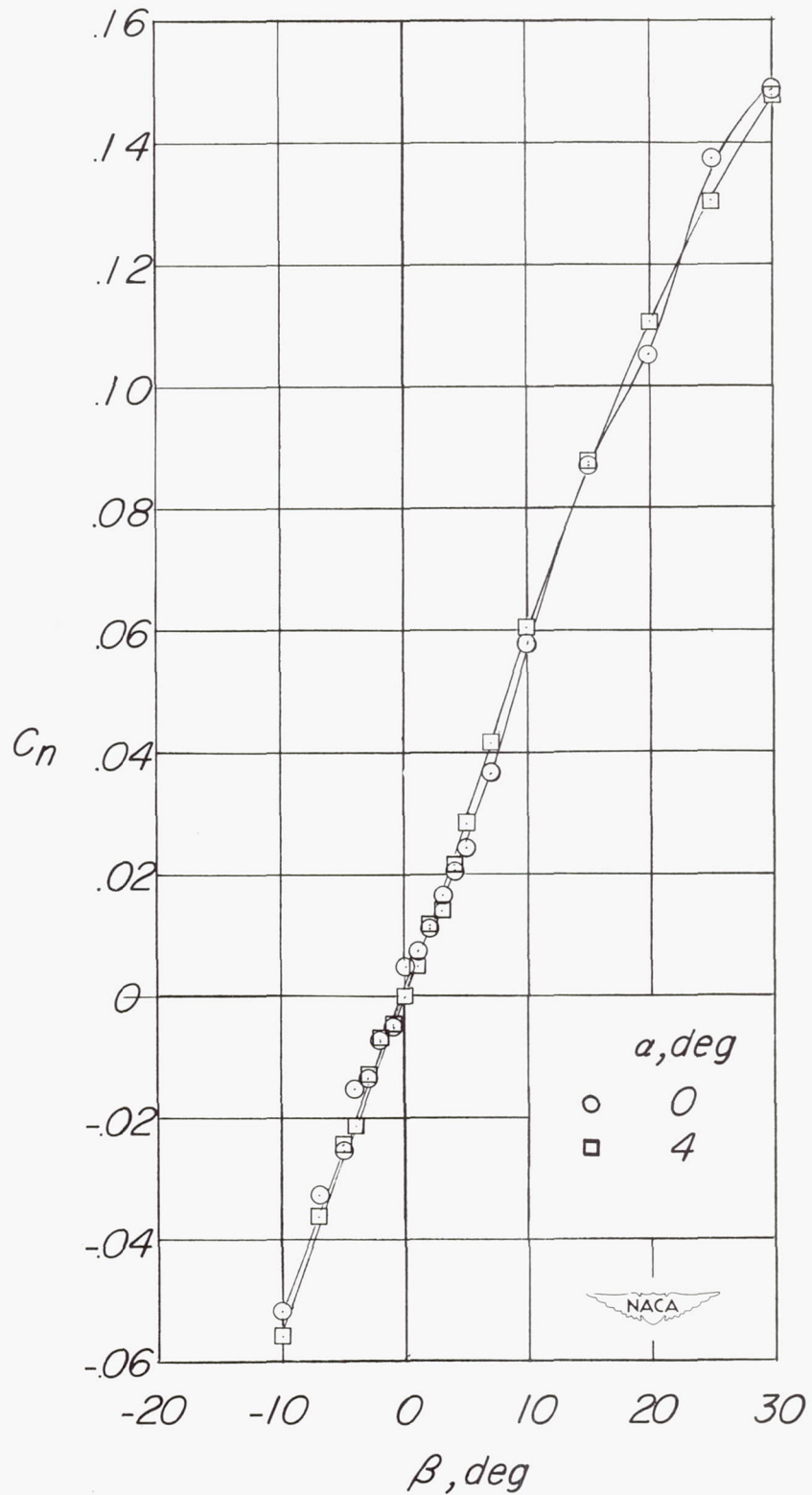


Figure 14.- Concluded.

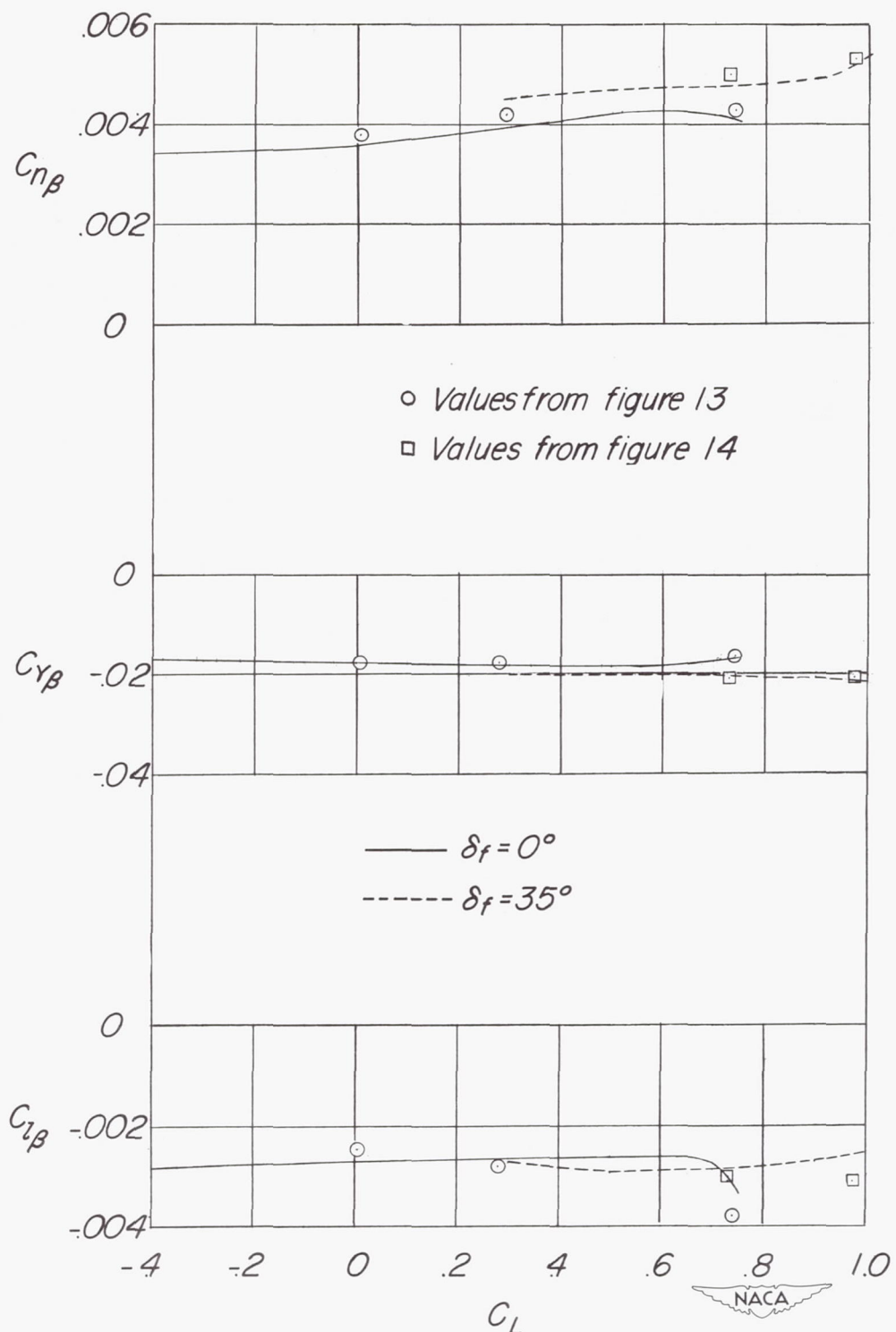


Figure 15.- Variation of static lateral stability parameters with lift coefficient of a 1/4-scale model of the Bell X-1 airplane equipped with a 4-percent-thick, aspect-ratio-4 wing.

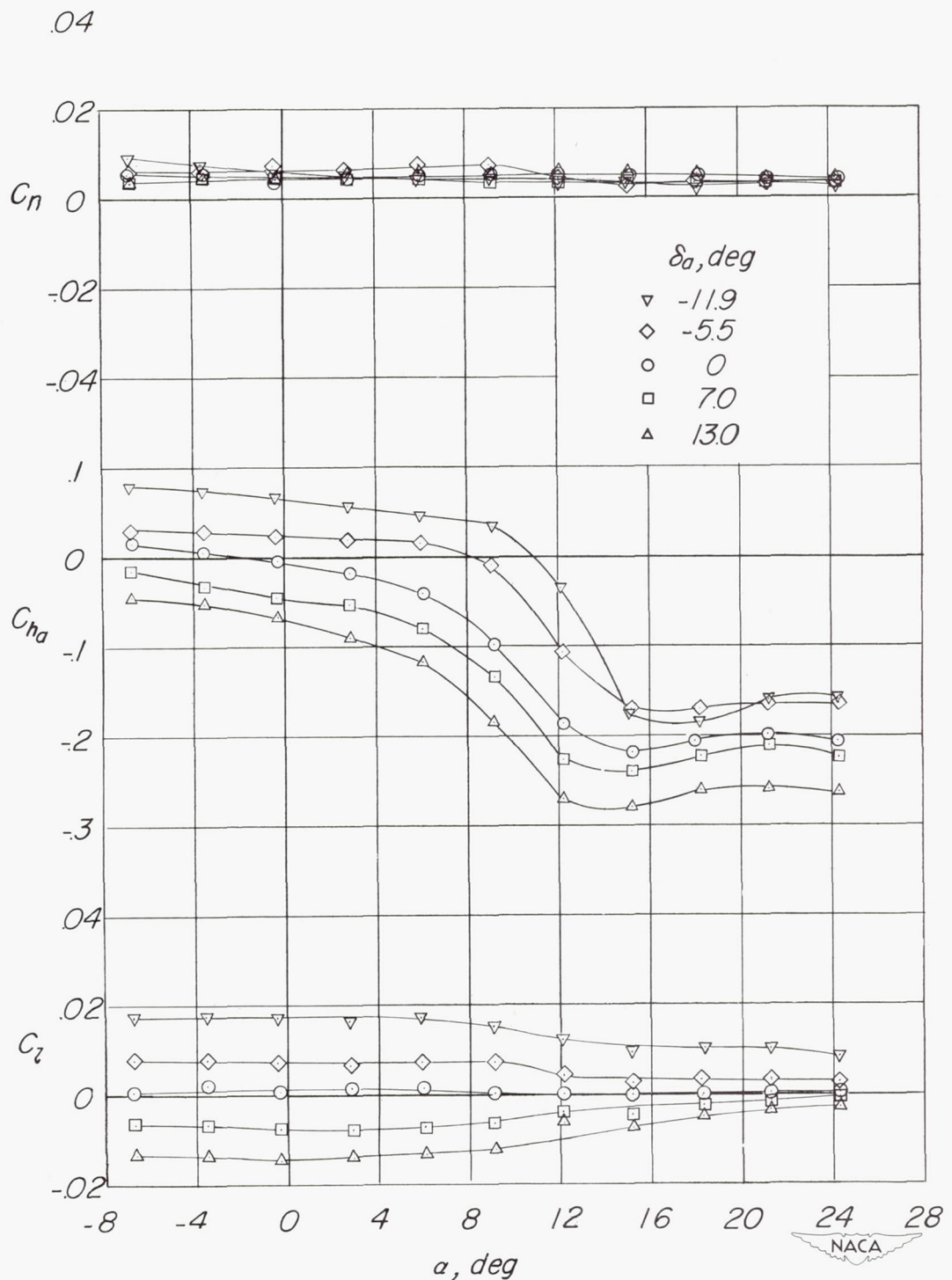


Figure 16.- Variation of the lateral control characteristics in pitch of a 1/4-scale model of the Bell X-1 airplane equipped with a 4-percent-thick, aspect-ratio-4 wing.  $\delta_f = 0^\circ$ ;  $i_t = 0^\circ$ ;  $\delta_r = 0^\circ$ ;  $\delta_e = 0^\circ$ .

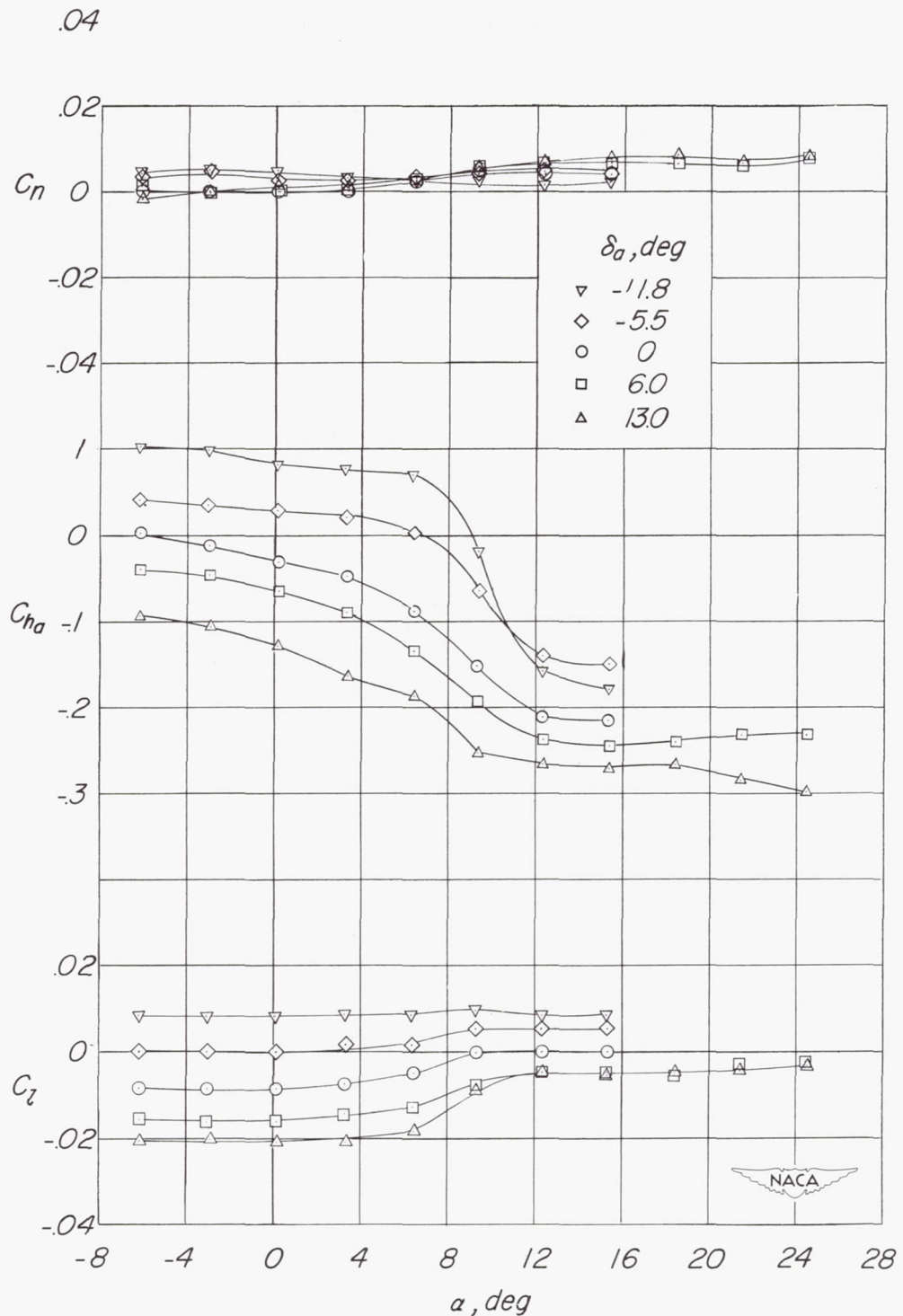


Figure 17.- Variation of the lateral-control characteristics in pitch of a 1/4-scale model of the Bell X-1 airplane equipped with a 4-percent-thick, aspect-ratio-4 wing.  $\delta_f = 35^\circ$ ;  $\delta_r = 0^\circ$ ;  $\delta_e = 0^\circ$ ;  $i_t = 0^\circ$ .

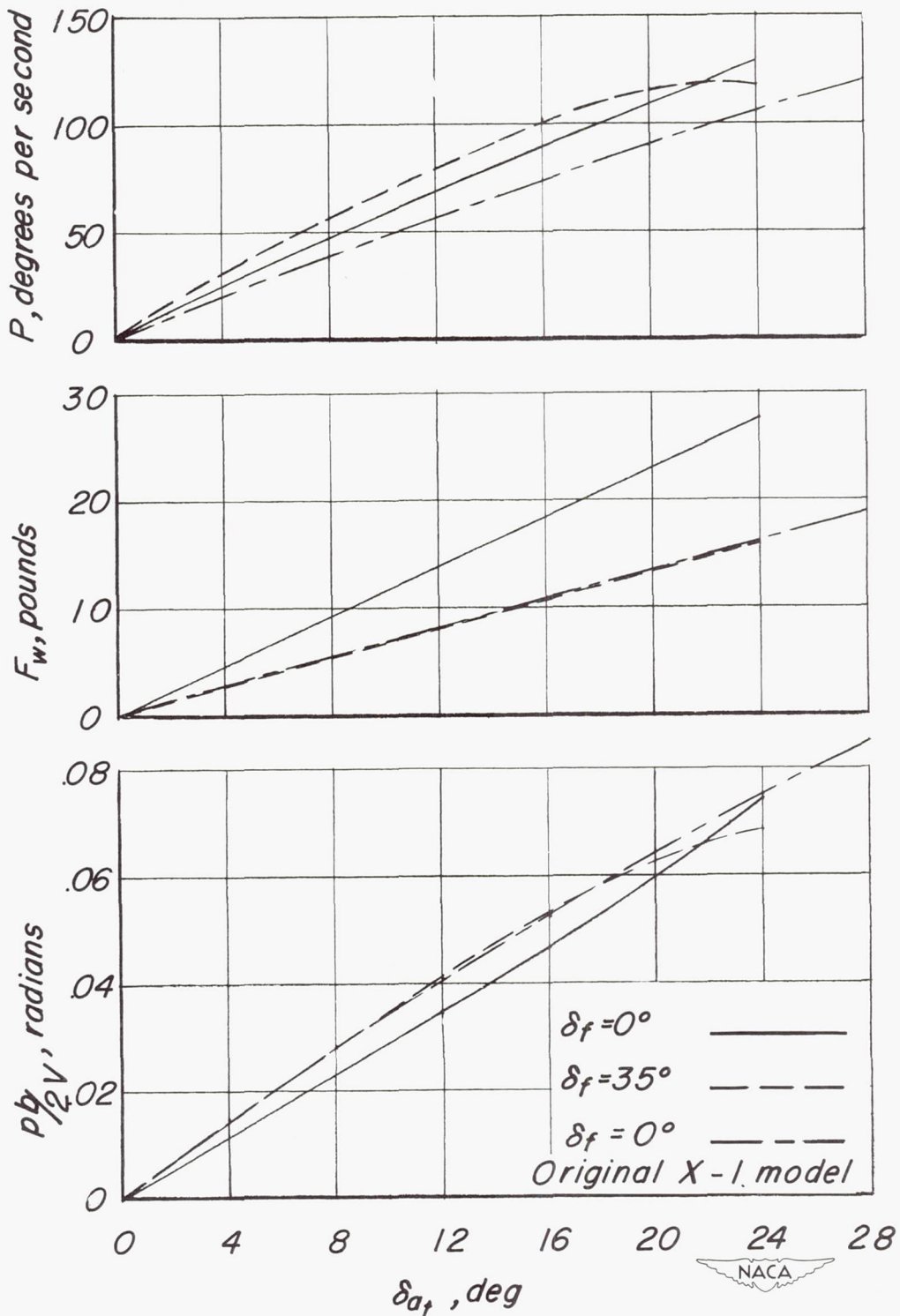


Figure 18.- Variation of helix angle, wheel force, and rolling velocity for steady roll. Conditions I and II for the model of the present investigation; condition I for the original X-1 model.

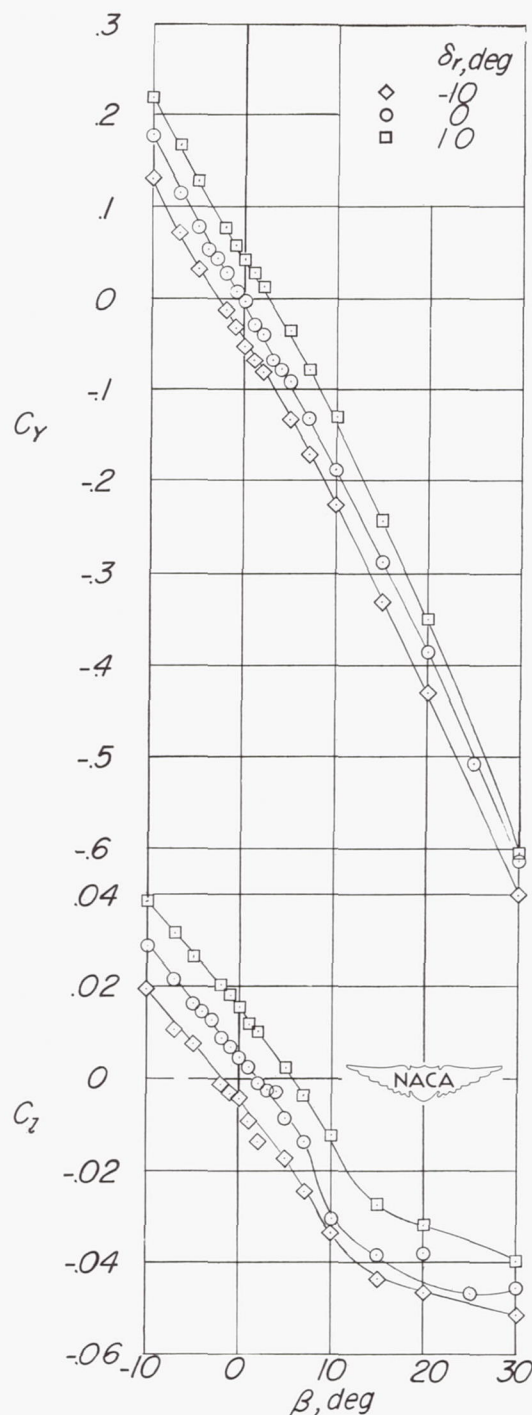
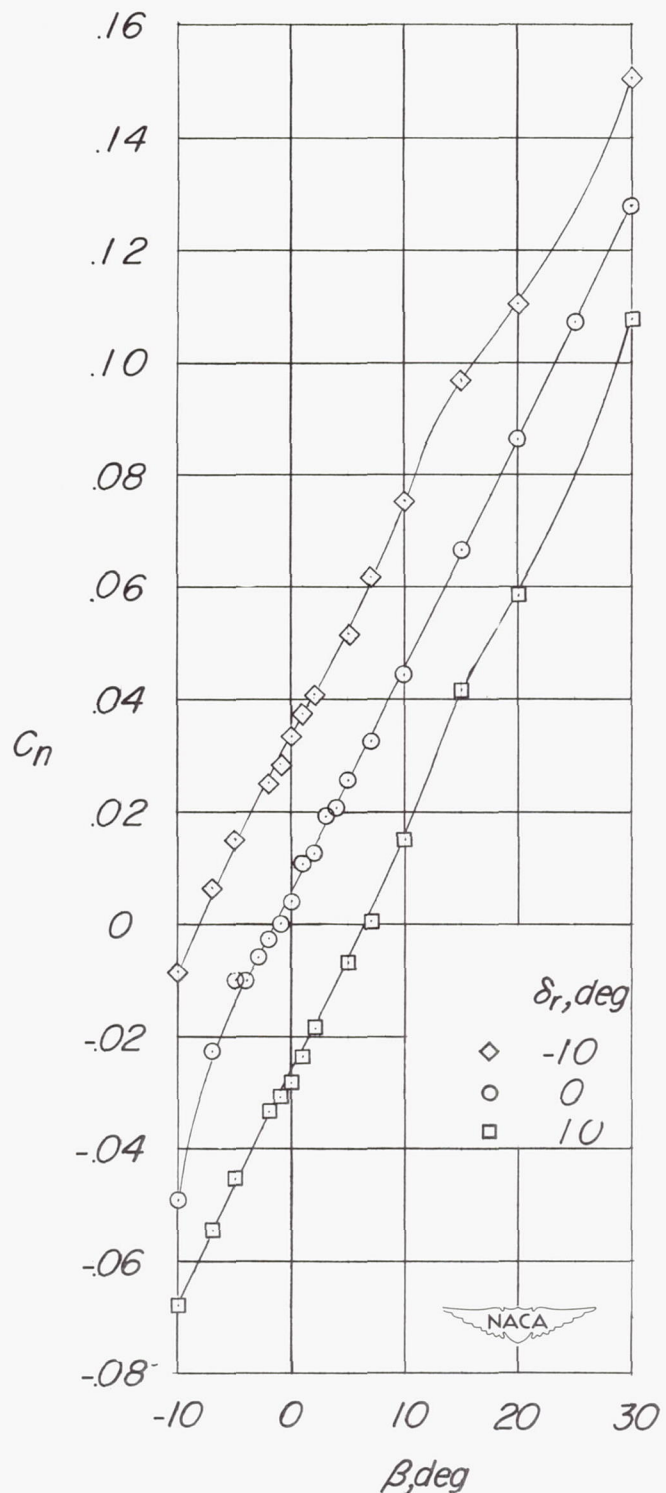
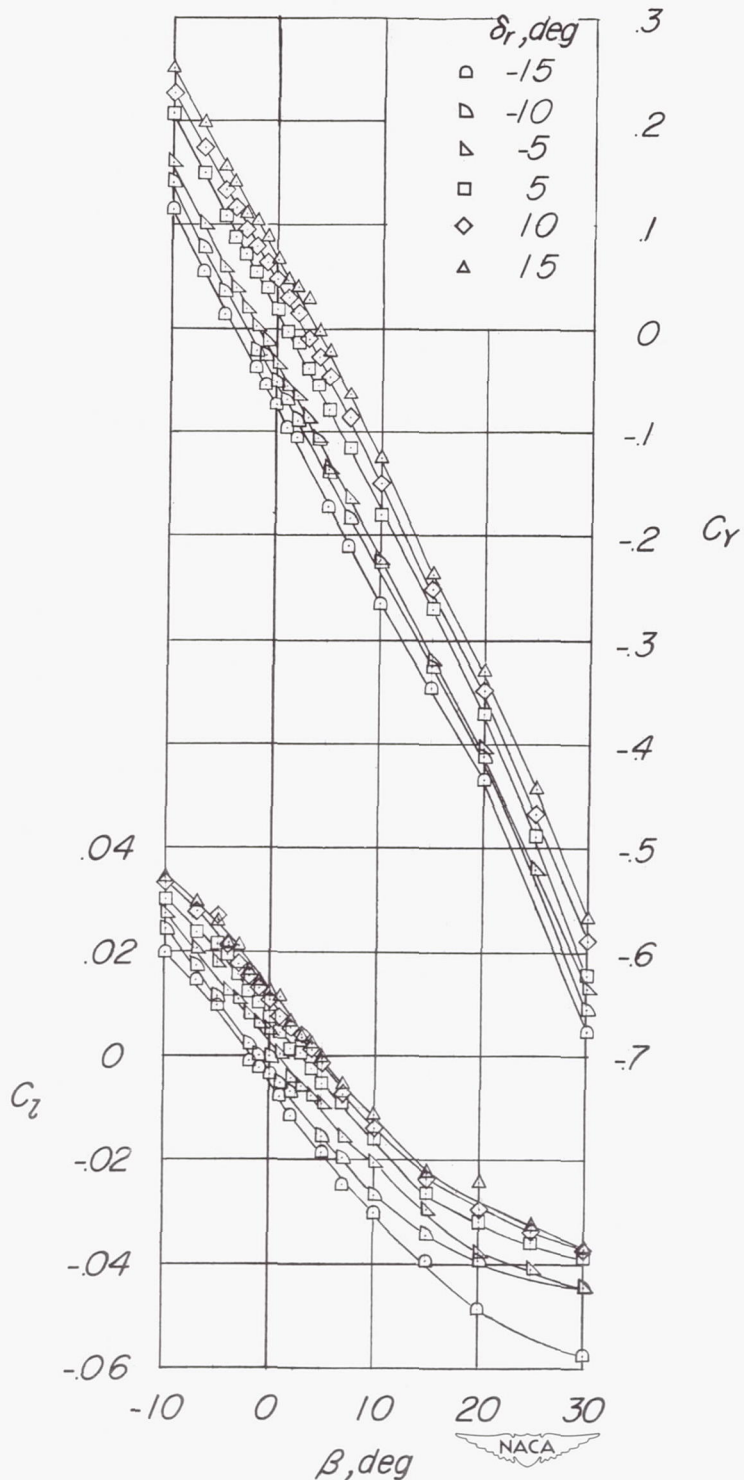
(a)  $\alpha = 0^\circ$ .

Figure 19.- Effect of rudder deflection on the aerodynamic characteristics in sideslip of a 1/4-scale model of the Bell X-1 airplane equipped with a 4-percent-thick, aspect-ratio-4 wing.  $i_t = 0^\circ$ ;  $\delta_f = 0^\circ$ .



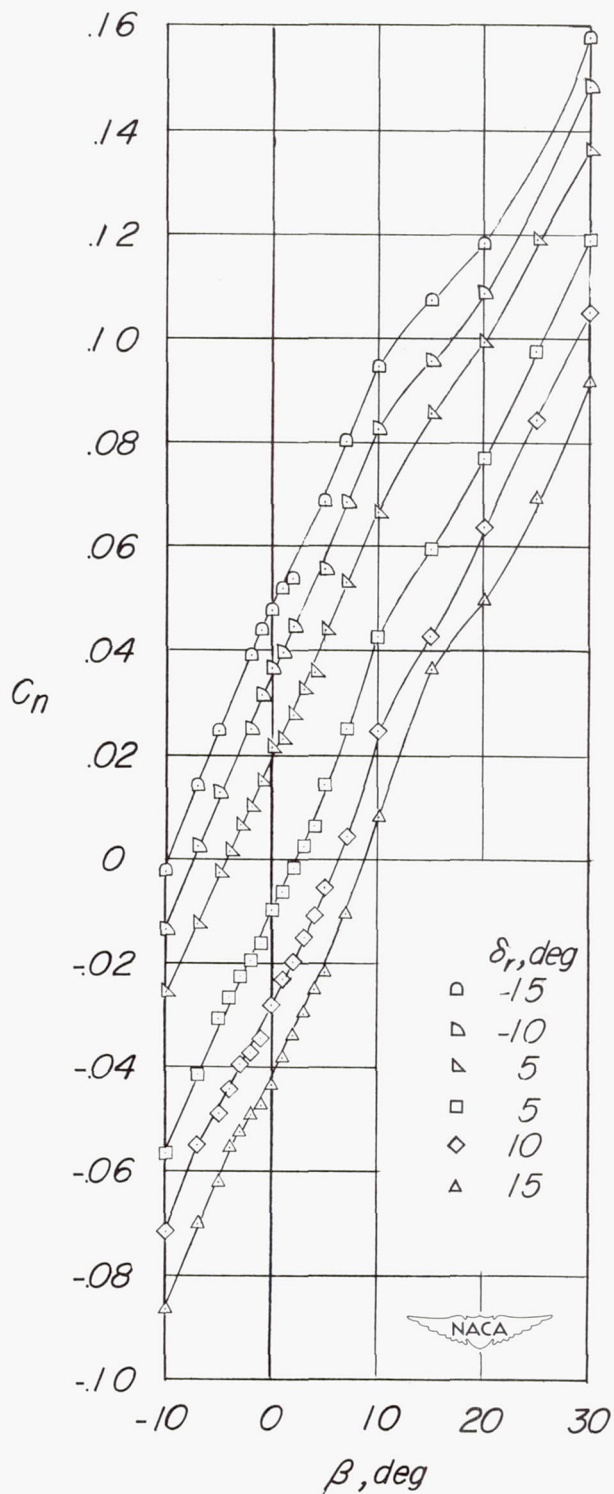
(a) Concluded.

Figure 19.- Continued.



(b)  $\alpha = 6^\circ$ .

Figure 19.- Continued.



(b) Concluded.

Figure 19.- Concluded.

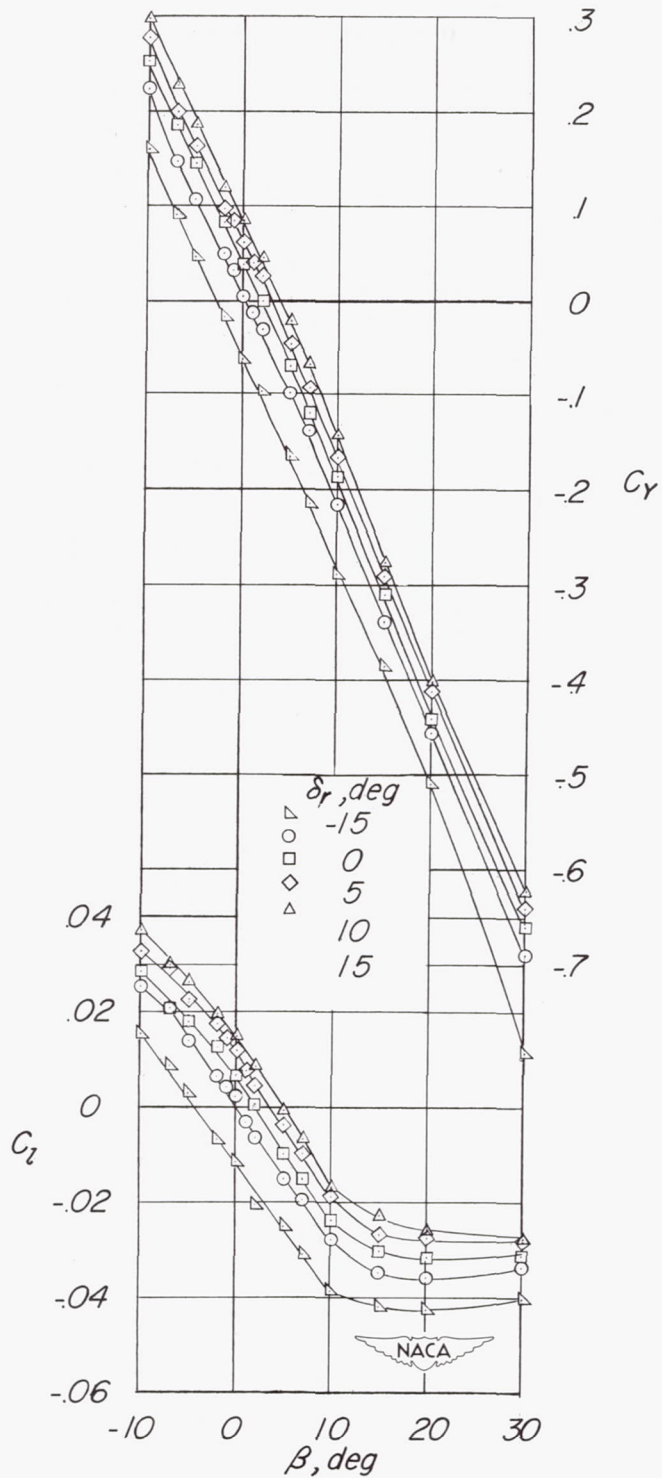


Figure 20.- Effect of rudder deflection on the aerodynamic characteristics in sideslip of a 1/4-scale model of the Bell X-1 airplane equipped with a 4-percent-thick, aspect-ratio-4 wing.  $\delta_f = 35^\circ$ ;  $\alpha = 4^\circ$ .

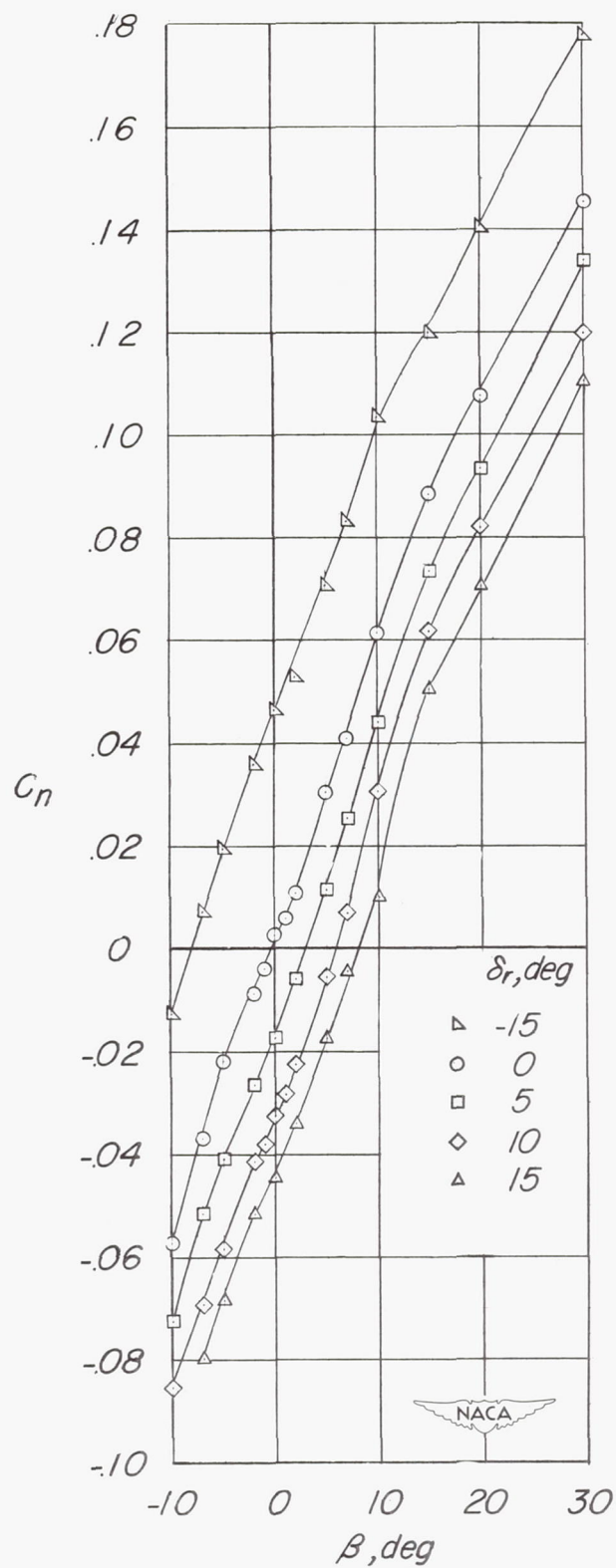


Figure 20.- Concluded.

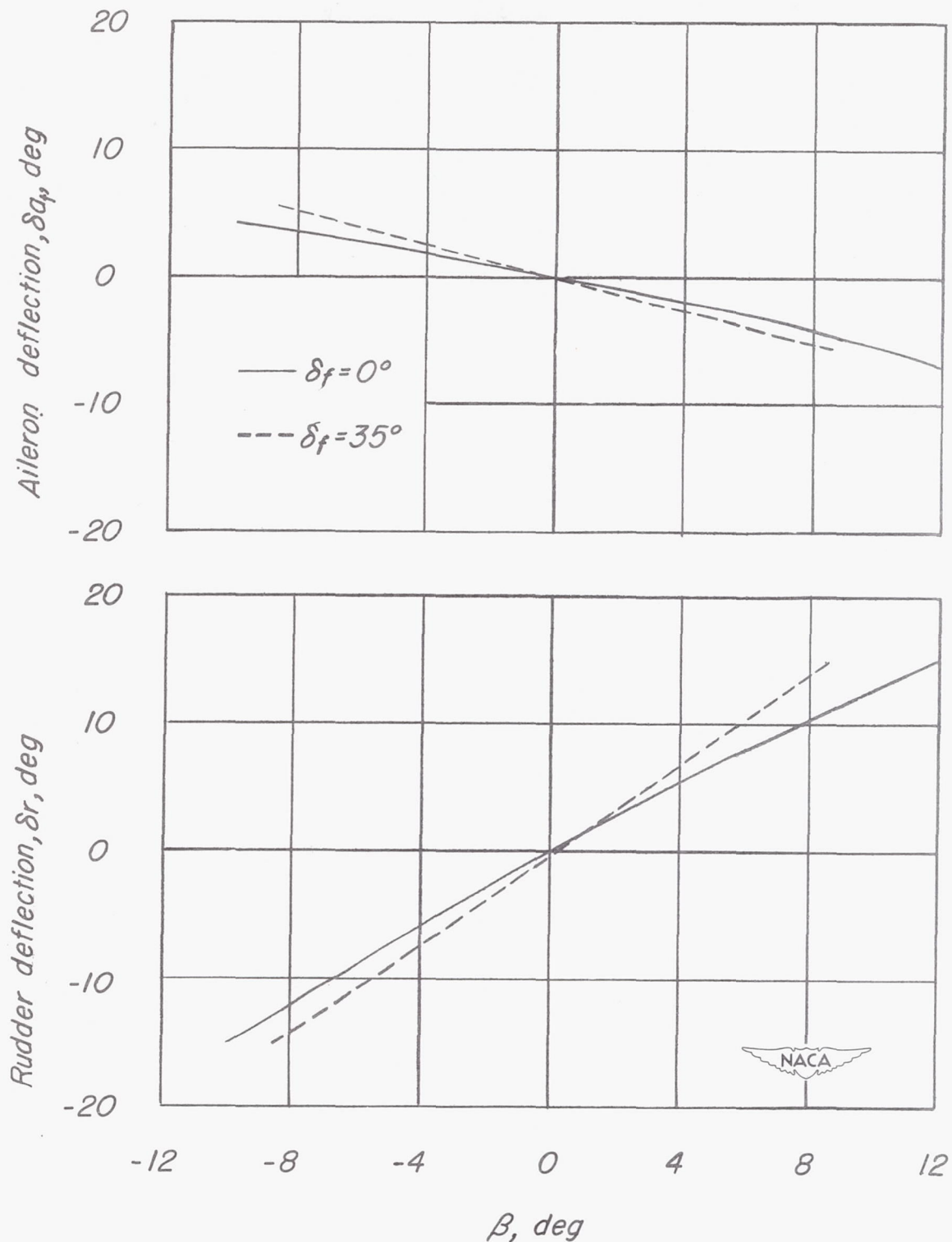


Figure 21.- Rudder and total aileron deflections required to maintain steady sideslip at low speed.

**SECURITY INFORMATION**  
**CONFIDENTIAL**

**CONFIDENTIAL**